ResearchGate

See discussions, stats, and author profiles for this publication at:
https://www.researchgate.net/publication/226555072

The Iron–Quinone Acceptor Complex

CHAPTER · DECEMBER 2004

DOI: 10.1007/1-4020-4254-X_9

CITATIONS
40

READS
9

2 AUTHORS, INCLUDING:

Antony R Crofts
University of Illinois, Urbana-Champaign

247 PUBLICATIONS **11,173** CITATIONS

SEE PROFILE

Available from: Antony R Crofts
Retrieved on: 15 January 2016

Chapter 8

The Quinone Iron Acceptor Complex

Vasili Petrouleas
Institute of Materials Science, NCSR 'Demokritos', 153 10 Aghia Paraskevi Attikis, Greece

Antony R. Crofts
Department of Biochemistry, 419 Roger Adams Lab, 600 S. Mathews Avenuw, and Center for Biophysics and Computational Biology, University of Illinois at Urbana-Champaign, Urbana, IL 61801, U.S.A.

Summary 2
I. Introduction 2
II. Probing the Iron-Quinone Complex Through the Iron Site 2
A. General 2
B. Ligand Exchange Reactions and Effects on the Q_A/Q_B Electron Transfer Rate 3
1. Nitric Oxide 3
2. Cyanide 4
3. Carboxylate Anions 5
4. Effects of the Iron Ligation on the Q_A/Q_B Electron Transfer Rate 5
C. Redox Properties of the Iron 6
D. Spin States of the Iron and the Semiquinone-Iron Magnetic Interactions 6
E. On the Role of the Iron 8
III. Organization of the Quinone Binding Sites: The Two-Electron Gate 9
A. Structural Models of the Quinone Sites 9
B. Mechanism of the Two-Electron Gate 12
1. Kinetic Models of the Two-Electron Gate 12
2. The pH Dependence of the Apparent Equilibrium Constant, K_{app} 14
3. Estimation of the Rate Constants for the Reactions Including the Protonated Species, and Proton-Uptake at the Q_B-site 15
4. The Second Order Rate Constant for Binding of Plastoquinone 16
5. The Pathway for Electron Transfer in Susceptible and Resistant Biotypes 16
6. Role of D1-Ser264 in the Mechanism of the Q_B-Site 16
C. Binding of Inhibitors and Exogenous Quinones at the Q_B-Site 17
D. Structural and Mechanistic Information from Mutagenesis Studies 18
1. Herbicide Resistant Strains of Chlamydomonas and Cyanobacteria 18
2. Specific Mutagenesis of Herbicide Resistance Sites in Synechocystis 19
3. Combinatorial Mutagenesis of a Conserved Span of the de Loop 19
4. Specific Mutagenesis of D1-His252 Shows an Important Role in H^+-Processing 20
5. Excision of Residues from the PEST Sequence of the **de**-Loop 21
6. Mutagenesis to Explore the Bicarbonate Effect 21
E. Effects of Occupation of the Q_B-site on the E_m for Q_A and on the Equilibrium Constants in the Two-Electron Gate 21

Both authors welcome correspondence, email: [1] vpetr@ims.demokritos.gr; [2] a-crofts@life.uiuc.edu

T. Wydrzynski and K. Satoh (eds): Photosystem II: The Water/Plastoquinone Oxido-Reductase in Photosynthesis, pp. 000–000.
© 2005 Kluwer Academic Publishers. Printed in The Netherlands.

F. Role of the Q_B-Site in Back-Reactions to the S-States 22
1. Back Reaction from Q_B^- to the S_2-State 22
2. Back Reaction from QH_2 to the S_3-State — A Possible Role for Cytochrome b_{559} 22
IV. Conclusions 23
Acknowledgments 23
References 24

Summary

The flux of reducing equivalents out of Photosystem II occurs through the two-electron gate function catalyzed by the iron-quinone complex on the acceptor side. The mechanism of the two-electron gate has been studied more completely in bacterial reaction centers, where an understanding of function has benefited from a structural context. However, the two-electron gate was discovered in green plants, and a large body of work had suggested that the mechanism and main structural features are similar in the two systems, and this is now confirmed by structures. In Photosystem II a number of additional properties are found, which result from the redox activity of the non-heme iron of the acceptor complex, and from the lability of its ligands. Pending structures for Photosystem II at a higher resolution, much of the discussion on the molecular architecture had borrowed the structural context from the bacterial homologue. One theme in this chapter is the justification for this borrowing that comes from the application of spectroscopic approaches to the Photosystem II acceptor complex. This has been especially successful in studies of the Q_A-site semiquinone, the magnetic interaction between the semiquinone formed at the site and the iron, and the interaction of external ligands with the iron. A second theme, reflecting the poor stability of the semiquinone of the Q_B-site in isolated Photosystem II preparations, is the use of indirect approaches, including kinetic studies and structural modeling, to understand the structure-function interface. The crystallographic structures now available provide a gratifying validation of these alternative approaches.

I. Introduction

The flux of reducing equivalents out of Photosystem II (PS II) occurs through the two-electron gate function catalyzed by the iron-quinone complex on the acceptor side. The complex consists of two plastoquinone molecules, Q_A and Q_B, separated by a non-heme iron(II) ion, and the protein milieu that houses these redox centers. The two quinones operate as sequential electron acceptors, Q_A being a one- and Q_B a two-electron acceptor. Electron transfer rates between the two quinones are of the order of a few tenths of a millisecond, but these vary depending on the treatment. Speculation about the spatial organization of the iron-quinone complex had been derived mainly from spectroscopic studies and protein-sequence comparisons with the bacterial reaction center (BRC) from *Rhodopseudomonas viridis* and *Rhodobacter sphaeroides*, now validated by crystallographic structures (see Fig. 1 for an overview). In the present chapter we avoid repeating topics that were extensively covered in earlier reviews (Crofts and Wraight, 1983; Rich and Moss, 1987; Diner et al., 1991; Diner and Babcock, 1996). Emphasis is rather given to selected aspects of the iron-quinone complex, the progress that has been made in recent years, and topics/views which were not adequately covered in the earlier reviews.

Abbreviations: Atrazine – 6-chloro-n-ethyl-N′-(1-methylethyl)-1,3,5-triazine-2,4-diamine; BRC – bacterial reaction center; Chl – chlorophyll; Cyt – cytochrome; D1, D2 – reaction center core subunits of PS II; DCBQ – 2,5-Dichloro-*p*-BQ; DCMU – 3(3,4-dichlorophenyl)-1,1-dimethylurea.; I. S. – Isomer Shift; NR – neutral red; *o*-phenanthroline – 1,10-phenanthroline; *p*-BQ – 1,4-benzoquinone; PDB – protein data bank; P-p-BQ – Phenyl-*p*-BQ; PQ – plastoquinone; PS II – Photosystem II; Q_A, Q_B, – the primary and secondary PQ acceptors of PS II; QSAR – Quantitative Structure Activity Relationship; UQ – ubiquinone

II. Probing the Iron-Quinone Complex Through the Iron Site

A. General

The iron located between the two quinones has strong spectral and structural similarities to the general class (not often recognized as such) of non-heme

mononuclear-iron centers found in oxygen-activating enzymes with diverse catalytic functions, including oxidations, mono- and di-oxygenations, and hydrations (Michel and Deisenhofer, 1988; Anderson et al., 1989; Diner et al., 1991; Lipscomb and Orville, 1992; Que et al., 1996; Feher and Okamura, 1999). Characteristic of this type of iron center is the flexibility of the iron coordination. The coordination number varies between 3 and 6 with the most common ligands being nitrogens (histidine-imidazole), and oxygens (carboxylate, phenolate, water). The variation in the ligand donor set modulates to a great extent the redox potential of the iron between extreme limits. A different number of labile ligands can be found in each case and this is linked to the specific catalytic function of the iron. Characteristic is the reversible binding of small molecules like nitric oxide and cyanide (Lipscomb and Orville, 1992; Orville and Lipscomb, 1997). Hegg and Que (1997) comparing the structures of a number of different enzymes catalyzing diverse reactions noted that, the common coordination feature in this type of iron centers is a 2-His-1-carboxylate facial triad. The occupation of the three remaining coordination sites by additional endogenous protein residues and/or exogenous ligands (e.g., substrate molecules) tunes to a great extent the properties of the metal center (Hegg and Que, 1997; Que, 2000). The iron of the BRC has perhaps the most inert coordination with 4 His plus a fixed glutamate bidentate ligand (Deisenhofer et al., 1985; Allen et al., 1988) and a high E_m (Beijer and Rutherford, 1987; Diner and Petrouleas, 1987b). Based on extensive spectroscopic and sequence homologies (Rutherford, 1987; Michel and Deisenhofer, 1988; reviewed in Diner et al., 1991), the iron of PS II is also assumed to be coordinated by four histidines, two from each of the two protein subunits D1 and D2. Compared to the BRC, there are important differences in the fifth and sixth coordination positions. At least one of these positions is occupied by bicarbonate in PS II (Diner and Petrouleas, 1990). According to FTIR studies, bicarbonate binds as a bidentate ligand in the reduced state of the iron (Fe^{2+}), and monodentate in the oxidized state (Hienerwadel and Berthomieu, 1995). The iron of PS II has at least two labile ligands and is redox active, as detailed below. These properties differentiate it from its bacterial counterpart, and suggest a more rich physiological function. The lability of the bicarbonate ligand probably explains certain heterogeneities associated with the iron-quinone complex.

B. Ligand Exchange Reactions and Effects on the Q_A/Q_B Electron Transfer Rate

In PS II, unlike the BRC where no lability of ligands has been reported, a number of molecules can bind reversibly at the non-heme iron site often in competition with bicarbonate, resulting in most cases in deceleration of the electron transfer.

1. Nitric Oxide

A direct demonstration of exogenous ligand binding to the iron has been provided by treatment with nitric oxide, which gives rise to a pronounced EPR signal at $g = 4.0$, characteristic of an iron-nitrosyl complex with $S = 3/2$ (Petrouleas and Diner, 1990). This is accompanied by an at least tenfold decrease of the electron transfer rate between Q_A and Q_B from the second saturating flash excitation onward (Diner and Petrouleas, 1990). The effects of NO are reversed by the addition of approximately 10 mM bicarbonate (Diner and Petrouleas, 1990). This suggests that bicarbonate is a labile ligand to the iron, confirming earlier predictions (Michel and Deisenhofer, 1988; van Rensen et al., 1988). Orientation studies of the $g = 4$ signal imply that NO, and by extrapolation one of the oxygens of bicarbonate, occupy a position homologous to one of the glutamate oxygens of the purple bacteria (Deligiannakis et al., 1992). Formate, an anion which also competes with bicarbonate (see below), binds simultaneously with NO, as it does not decrease the Fe^{2+}-NO signal but it changes somewhat its rombicity (Diner and Petrouleas, 1990). Direct evidence for the simultaneous binding of NO and another anion to the iron, has been provided by the observation of pronounced superhyperfine structure on the $g = 4$ signal from the fluoride nucleus, under the simultaneous presence of NO and F^- (Sanakis et al., 1999). NO and F^- have been suggested to bind cis to each other in a hexa-coordinate arrangement (Sanakis et al., 1999). It is reasonable to assume that NO and formate bind in a similar fashion. Experiments with oriented membranes (Hanley and Petrouleas, unpublished) show that the orientation of the $g = 4$ signal principal axes does not change (except for an interconversion of the x and y axis) in the presence of fluoride. This and the fact that the added anions do not alter significantly the spin Hamiltonian parameters of the Fe^{2+}-NO $S = 3/2$ configuration strongly suggests that the iron-NO complex in the absence of exogenous anions is also hexa-coordinate. It is

possible that at the initial stages of bicarbonate displacement, bicarbonate binds simultaneously with NO as a monodentate ligand. Full displacement of bicarbonate (and replacement, for example, by water) is probably facilitated by the reduction of Q_A^-, as the experiment described below suggests. This would offer a possible explanation of the observation mentioned above, that the NO-induced deceleration of the electron transfer develops fully from the second flash and onward (Diner and Petrouleas, 1990). It could also explain the small modification (small increase in rombicity) of the Fe^{2+}-NO EPR signal following the first illumination/dark-adaptation cycle in a series of cycles effecting successive electron transfers among the quinones (Petrouleas and Diner, 1990).

Recently a new mode of transient binding of NO to the iron has been reported. The affinity for this mode of binding is enhanced by the reduction of Q_A (Goussias et al., 2002). The new transient state is trapped at –30 °C and is characterized by EPR signals with *g* values of 2.016 in the presence of NO alone or 2.027 and 1.976 in the simultaneous presence of NO and CN^-. An important implication of the results is a trans influence of Q_A reduction on the bicarbonate ligation to the iron. This is transmitted presumably via hydrogen-bonding (H-bonding) of Q_A with an imidazole ligand to the iron. In the absence of CN^-, NO has been concluded to bind in a 5-coordinate geometry, under these conditions.

Prolonged incubation with NO appears to result in a dinitrosyl-iron species (Goussias et al., 2002). Reduction by free NO explains probably the appearance of weak EPR signals in dark-adapted material very similar to a synthetic $Fe(NO)_2$(imidazole) species, but full evolution of the signal is effected by illumination. Presumably Q_A^- reduces the dinitrosyl complex under these conditions.

The proposed iron coordination in the presence of NO and the various anions is summarized in Scheme 1.

2. Cyanide

Cyanide, binds stepwise (Koulougliotis et al., 1993; Sanakis et al., 1994). With an approximate K_d of 10-20 μM, it eliminates the $g = 4.0$ signal induced

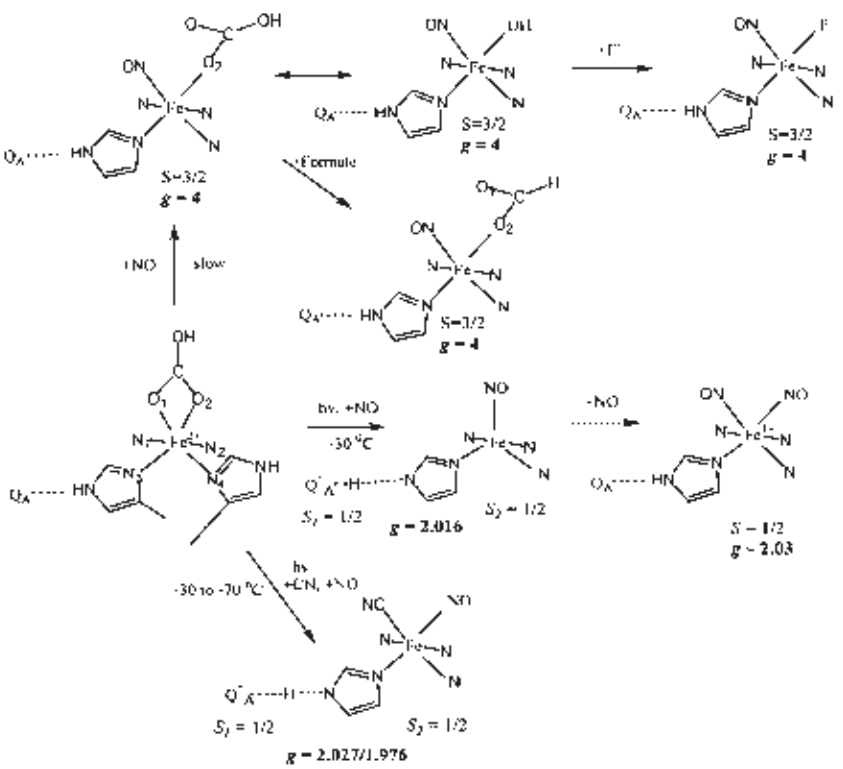

Scheme 1. Suggested modes of NO binding to the iron.

by NO. At higher concentrations, K_d 0.1-0.2 mM, CN^- causes a shift of the $Q_A^-Fe^{2+}$ signal to $g = 1.98$ and modifies the split-pheophytin signal (Sanakis and Petrouleas, 1995), and with an approximate K_d of 1.2 mM it converts the iron to low spin ($S = 0$) (Sanakis et al., 1994). The cyanide experiments imply that up to three sites at (or near) the non-heme iron are accessible to exogenous ligands. The data do not provide direct evidence that all cyanides bind as iron ligands, since binding in the vicinity of the iron could explain some of the effects. It is expected, however, that conversion of the iron ion to its low spin form would require the binding of more than one CN^- ligand. This is corroborated by FTIR studies, which reveal at least two CN^- bands in the Q_A^-/Q_A spectra (Noguchi et al., 1999a). The effects of cyanide can be reversed by prolonged storage in a cyanide free medium at pH 6 (Sanakis et al., 1994).

3. Carboxylate Anions

Apart from NO and cyanide, a number of carboxylate anions appear to bind at the non-heme iron in apparent competition with bicarbonate. Formate (in particular) and acetate have been studied extensively in the past as competitive inhibitors of bicarbonate (Robinson et al., 1984; Stemler and Murphy 1985; Eaton-Rye and Govindjee 1988). The extension of the studies to a series of carboxylate anions (e.g. glycolate, glyoxylate, oxalate, and lactate) (Deligiannakis et al., 1994; Petrouleas et al., 1994) has yielded important new insights onto the mode of action of the carboxylate ligands to the iron. The anions compete with NO for binding to the iron (Deligiannakis et al., 1994) implying that they bind as bidentate ligands. Formate, the smallest of the carboxylate anions appears to be the only exception, binding simultaneously with NO (see Section II.B.1). Difference (Fe^{2+}/Fe^{3+}) FTIR spectroscopy with ^{12}C- and $^{13}C_1$-labeled lactate indicates that this anion binds through one carboxylate oxygen and the hydroxyl group in both oxidation states of the iron (Berthomieu and Hienerwadel, 2001). Glycolate, an anion that has a similar effect with lactate on the Fe^{3+} EPR spectra (Deligiannakis et al., 1994) and on significantly lowering the midpoint potential of the iron (discussed below), is inferred to bind in a similar fashion (Berthomieu and Hienerwadel, 2001).

4. Effects of the Iron Ligation on the Q_A/Q_B Electron Transfer Rate

Of all the molecules that bind at the iron site bicarbonate appears to be unique (with the possible exception of cyanide, whose effects on the electron transfer rate are not fully understood, Koulougliotis et al., 1993) in supporting an undiminished electron flow in the iron-quinone complex. Replacement with formate is well known to induce a pronounced slowing of the electron transfer rate; a three- to four-fold slowing on the first flash, and a ≥tenfold slowing on subsequent flashes (Robinson et al., 1984; Snel and van Rensen, 1984; Eaton-Rye and Govindjee, 1988). NO has a similar effect (Diner and Petrouleas, 1990). Among the various carboxylate anions examined, glycolate has a similar pronounced effect and notably it exerts its effects at a concentration at least 3-fold lower than that of formate with a K_m of 0.5–0.7 mM at pH 6.3 (Petrouleas et al., 1994). Glyoxylate and oxalate induce less pronounced effects (Petrouleas et al., 1994). It has been suggested that bicarbonate plays a role in the protonation of Q_B (Stemler and Murphy, 1985; van Rensen et al., 1988; Diner et al., 1991). The parallel effects of the various anions on the midpoint potential (and its pH dependence) of the iron (see below), the $Q_A^-Fe^{2+}$ EPR signals (see below), and the Q_A/Q_B electron transfer rate, could be explained if we assume that, binding of the anions to the iron modifies the pK_a of a nearby group(s) involved in the protonation of Q_B (Nugent et al., 1988; Deligiannakis et al., 1994, Petrouleas et al., 1994). Insights are offered by FTIR studies, which indicate a hydrogen-bond network from the non-heme iron toward the Q_B pocket involving bicarbonate and D1- His215 (Berthomieu and Hienerwadel, 2001). Independent support of these suggestions comes from the counter effect that Q_A reduction has on the bicarbonate ligation (detected by the use of NO) transmitted via the H-bonding of D2-His 215 to Q_A^- (Goussias et al., 2002; see Scheme 1). The symmetric shape and binding of the bicarbonate molecule, the pK_a of its protonatable groups together with its size could be critical factors in the support of its proposed role. When bicarbonate is exchanged by other molecules, e.g.. NO, an alternative slow proton pathway may function. As however, according to scheme 1, bicarbonate may still remain bound as a monodentate ligand until after the reduction of Q_A by a first flash in a flash series, the protonation-limited slowing of the electron transfer appears after the second flash.

It is possible that certain anions whose effect on the electron transfer rate is moderate (e.g. glyoxylate), can substitute in part for bicarbonate or affect the pK_a values of protonatable groups along the proton translocation pathway.

C. Redox Properties of the Iron

The interesting redox properties of the iron have been reviewed extensively in the past (Diner and Petrouleas, 1987b). Briefly, the Fe^{3+}/Fe^{2+} couple has been identified as the Q_{400} electron acceptor (Ikegami and Katoh, 1973) with a midpoint potential of about 400 mV at pH 7 that varies by approximately –60 mV per pH unit between pH 5.3 and 8.5 (Bowes et al., 1979a; Petrouleas and Diner, 1986). This potential is rather high for participation of the iron in electron transfer reactions. Once the iron is oxidized, however, Q_A^- reduces it rapidly ($t_{½}$ = 7 μs at pH 6.5, reviewed in Diner and Petrouleas, 1987b). On the other hand a number of exogenous quinones (e.g. *p*-BQ, P-*p*-BQ, and DCBQ) acting through the Q_B site can oxidize the iron, once reduced by Q_A^- to the semiquinone form (Zimmermann and Rutherford 1986; Petrouleas and Diner, 1987a,b). The carboxylate anions that compete with bicarbonate for binding at the iron modify significantly the redox properties of the iron (Deligiannakis et al., 1994). Glycolate and lactate lower the midpoint potential to 340 mV and make it pH-independent, while oxalate, malate and formate induce midpoint potentials higher than 500 mV in the pH range 6.1 to 7.5. Glyoxylate and pyruvate have intermediate effects. The effect of these anions has being attributed to the shift of the pK_a of an ionizable group that is responsible for the pH dependence of the midpoint potential of the iron. Molecules that bind at the Q_B site (DCMU, *o*-phenanthroline, atrazine, P-p-BQ) appear to raise to a variable extent the midpoint potential of the iron. Oxidation of the iron, on the other hand, lowers the affinity for binding at the Q_B site (Wraight, 1985).

D. Spin States of the Iron and the Semiquinone-Iron Magnetic Interactions

The iron can attain a variety of spin states following a number of reversible treatments.

S = 5/2, obtained in the Fe^{3+} state. The EPR spectra are characterized by resonances at g = 8.15, 5.63, 3.51 (Petrouleas and Diner, 1986) assigned to a system with parameters, D = 2–3 K, E/D = 0.11 (Diner and Petrouleas, 1987b; Aasa et al., 1989). Binding of exogenous molecules at the Q_B site reduces the E/D value resulting in some cases in axial spectra (Itoh et al., 1986; Diner and Petrouleas, 1987a,b). Orientation studies indicate that the g_y axis runs along the homologous direction of the bacterial twofold symmetry axis (Deligiannakis et al., 1992). The g_z axis is inferred to lie along the N-Fe-N direction defined by the nitrogen ligands from the histidines not participating in the binding of the two quinones. Photoreducible high-spin iron signals initially attributed to heme iron have been now assigned to the non-heme iron of the acceptor side (Nugent, 2001). Carboxylate molecules bound on the iron exert small effects on the D parameter but some of the anions induce resonances at g = 4.3 corresponding to D = 0.7 K and E/D = 0.315 (Deligiannakis et al., 1994). No evidence for the trapping of the intermediate $Q_A^-Fe^{3+}$ has been presented. It is possible, however, that the light-induced decrease of the Fe^{3+} signal at 77 K and lower temperatures (Diner and Petrouleas, 1987b; Nugent, 2001) may be due to the alteration of the Fe^{3+} signal by the magnetic interaction with Q_A^- rather than the reduction of the Fe^{3+}, which may be limited by the uptake of a proton.

S = 2, natural state (Fe^{2+}) in the majority of centers. No EPR signals have been reported for this integer-spin state, but Mossbauer spectroscopy has provided valuable information (reviewed in Debrunner, 1996). Useful insights have been provided by comparison with a series of synthetic model compounds (Boinnard et al., 1990; Garge et al., 1990; Rakotonandrasana et al., 1991; Martinez Lorente et al., 1995). The Mossbauer spectra in BBY preparations are heterogenous containing at least two components assigned to the non-heme iron with a common isomer shift of 1.19 mm/s and quadrupole splittings 2.07 mm/s (comp.1), and 2.99 (comp. 2) (Petrouleas et al., 1992). Component 2 appears to be the dominant one in most preparations (Petrouleas et al., 1992; Picorel et al., 1994; Garbers et al., 1998). In preparations from *Chlamydomonas reinhardtii* a single component with a similar isomer shift but an average quadrupole splitting was observed (Petrouleas and Diner, 1982). The isomer shift in all cases indicates octahedral coordination with oxygens or nitrogen ligands, as was originally suggested for the homologous iron in *R. sphaeroides* R-26 (Debrunner et al., 1975; Boso et al., 1981). Treatment with formate converts all of the absorption area to a component 1 type spectrum (Diner and Petrouleas 1987b; Semin et al., 1990; Pe-

trouleas et al., 1992). In the reduced state, the primary quinone, Boinnard et al., 1990; (S = ½), interacts magnetically with the non-heme iron (S = 2). This results in a severe broadening of the EPR spectrum of the semiquinone and the appearance of heterogenous features in the g 1.6 – 1.9 region of the EPR spectra (Nugent et al., 1981; Rutherford and Zimmermann, 1984, Nugent et al., 1992) with pronounced anisotropy (Rutherford, 1985). Notable is the pH dependent equilibrium between the '1.9' and the '1.84' form of the $Q_A^-Fe^{2+}$ signal (Rutherford and Zimmermann, 1984) and the dramatic enhancement by formate of the g = 1.84 form of the $Q_A^-Fe^{2+}$ signal (Vermaas and Rutherford, 1984). A correlation appears to exist between component 1 in the Mossbauer spectra, the g = 1.84 form and the non-oxidizable configuration of the iron (Petrouleas et al., 1992; Deligiannakis et al., 1994). The smaller quadrupole splitting value of component 1 (Petrouleas et al., 1992), as well as of the bacterial Fe^{2+} (Debrunner et al., 1975; Boso et al., 1981), has been assigned to a radial expansion of the 3d electrons of the iron, an effect that would stabilize the Fe^{2+} oxidation state, as observed experimentally. Apart from formate a number of carboxylate anions substituting for bicarbonate appear to support either the '1.9' or the '1.84' configuration (Deligiannakis et al., 1994). The pH-dependent heterogeneity in the presence of bicarbonate alone and the changes induced by the various carboxylate anions have been attributed to the shift of the pK_a of a critical ionizable group (Deligiannakis et al., 1994), possibly His D1-215 (Berthomieu and Hienerwadel, 2001). Cyanide at moderate concentrations induces an entirely new $Q_A^-Fe^{2+}$ EPR signal with pronounced intensity at g = 1.98 (Koulougliotis et al., 1993). The shift of the signal close to g = 2.0 must be due primarily to changes in the zero-field splitting of the iron(II) .

EPR signals in the g = 1.8 to 1.9 region have been also reported for the $Q_B^-Fe^{2+}$ state (Heathcote and Rutherford, 1987; Hubbard et al., 1989). A prominent EPR signal at g = 1.66 has been detected from the state $Q_A^-Fe^{2+}Q_B^-$ (Hallahan et al., 1991).

S = 3/2, obtained by the binding of NO to the iron. The EPR spectra are characterized by a prominent derivative at g = 4, indicative of axial symmetry with a small rhombicity (Petrouleas and Diner, 1990). The respective spin Hamiltonian parameters are, D = 10 ± 2 cm^{-1} and E/D = 0.013 and these change slightly following the simultaneous binding of formate (Diner and Petrouleas, 1990) or fluoride (Sanakis et al., 1999). In the presence of fluoride the parameters become D = 8 cm^{-1} and E/D = 0.025, as determined by the simulation of the EPR spectra at two different microwave frequencies, X and Q band (Sanakis et al., 1999). Studies of oriented spinach membranes treated with NO show that g_x lies on the membrane plane while g_y is oriented at 30° and g_z at 60° with respect to the membrane plane (Deligiannakis et al., 1992). A similar axes orientation is observed in the simultaneous presence of F^- (Hanley and Petrouleas, unpublished). The simultaneous binding of NO and fluoride to the iron induces prominent hyperfine splitting of the g = 4 resonance from the fluoride nucleus (I = ½). Following reduction of Q_A the system of the two half-integer interacting spins (½ for the semiquinone and 3/2 for the iron-NO complex) does not have detectable resonances at X-band frequencies but it has resonances at Q band. In the simultaneous presence of fluoride, however, prominent resonances with components in perpendicular and parallel mode EPR at X- and Q-band frequencies are observed. The system of the two half-integer interacting spins has been successfully simulated with an antiferromagnetic-coupling constant of 0.5 cm^{-1} in the presence, and 1.3 cm^{-1} in the absence of F^- (Sanakis et al., 1999). No isotopic effect (^{14}NO-Fe vs ^{15}NO-Fe) could be detected in the CW EPR and ESEEM spectra, indicating that the spin density on the nitrogen nucleus of NO is very small (Deligiannakis et al., 1998). The coupling to three or four imidazole nitrogens could be detected by the application of the Hyscore spectroscopy, yielding the first spectroscopic evidence supporting histidine ligation to the iron (Deligiannakis et al., 1998).

S = ½, obtained under variable conditions. These conditions are: (*i*) chemical oxidation of the iron in the presence of high concentrations of cyanide (2 or 3 cyanide ions bound on the iron) (Sanakis and Petrouleas, 1995). The EPR spectra are characterized in this case by weak resonances at g_x = 2.60 and g_y = 2.33. (*ii*) binding of NO or NO and CN in the presence of the reduced Q_A at –30 °C (Goussias et al., 2002). New $Q_A^-Fe^{2+}$ EPR signals appear in this case at 2.016, presence of NO alone, or 2.027, 1.976 in the simultaneous presence of NO and CN^- and unlike all other signals from the complex (with the exception of the free semiquinone signal) the signals saturate at very low microwave power. Electron Spin Echo Envelope Modulation (ESEEM) experiments show the existence of two protein ^{14}N nuclei coupled to electron spin. These two nitrogens have been detected consistently in the environment of the semiquinone

Q_A^- in a number of PS II preparations. The signals can be simulated with the assumption of a $S = ½$ state of the iron-NO(CN) complex interacting with the semiquinone radical with aniferromagnetic J values in the range 0.025 t0 0.05 cm^{-1} (Goussias et al., 2002). (*iii*) binding of two NO molecules on the iron. One-electron reduction of this dinitrosyl species yields a half integer configuration characterized by g values of 2.05, 2.03, 2.01 (Goussias et al., 2002).

S = 0, diamagnetic state of the iron. This state is obtained in the presence of high concentrations of cyanide (2 or 3 cyanide ions bound on the iron) and is characterized by Mossbauer spectra with isomer shift = 0.26 mm/s and quadrupole splitting = 0.36 mm/s (Sanakis et al., 1994). The conversion of the iron to a diamagnetic form has allowed the observation and study of the unperturbed semiquinone radical at $g = 2.045$ (sse below). Mossbauer experiments in a PS^- mutant from *C. reinhardtii* (Burda et al., 2003) indicated that the non-heme iron in these preparations occurs naturally in a low spin form.

The free semiquinone, Q_A^-, radical. Apart from the reversible conversion of the iron to $S = 0$ by cyanide (Sanakis et al., 1994), Q_A^- can be decoupled from the iron by treatments extending an original method of Klimov et al. (1980), including trypsinization (Macmillan et al., 1990) or replacement of the iron with the diamagnetic Zn^{2+} (Astashkin et al., 1995) (the binding of Zn^{2+} has not been demonstrated under these conditions), or by treatment of core complexes from *Synechocystis* with high concentrations of phosphate on the hydroxyapatite column (Tang et al., 1995), or by a high pH treatment (Deligiannakis et al., 1997). Probably all these treatments (except for the cyanide treatment) result in removal of the iron (Kurreck et al., 1996; Deligiannakis et al., 1999). The decoupled Q_A^- is characterized at X-band EPR by a 9.5 G wide derivative at $g = 2.0045$ (Sanakis et al., 1994) with resolved anisotropy at Q-band EPR and an unusually large g_{xx} component indicating weaker hydrogen bonds compared with plastosemiquinone in solution and possible π-interaction with aromatic amino acid residues (MacMillan et al., 1995a). The application of ^{1}H-ENDOR spectroscopy (MacMillan et al., 1995b; Rigby et al., 1995; Zheng and Dismukes, 1996) has provided useful information about the orientation of the hydrogen bonds and has indicated an asymmetry in the H-bonding. ESEEM spectroscopy detected coupling of the semiquinone electron spin to protein nitrogens (Astashkin et al., 1995; Deligiannakis et al., 1995, 1997; MacMillan et al., 1995a; Tang et al., 1995; Astashkin et al., 1998; Deligiannakis et al., 1999). These studies have been extended to intact preparations in which the iron is in its high-spin form (Peloquin et al., 1999). Apart from variations attributed to the effects of the different treatments and the pH, the experiments agree generally on the presence of two interacting nitrogen nuclei. These have been assigned to D1-Ala261 and D1-His215 (Astashkin et al., 1995; Deligiannakis et al., 1997), but this is contested by Peloquin et al. (1999) based on site directed mutagenesis and earlier His-labeling studies (Tang et al., 1995). It is generally agreed however that H-bonding between D1-His215 and Q_A^- exists (although its spectroscopic signature is not agreed upon), as suggested by FTIR studies (Noguchi, 1999a, b), too, and by analogy with the arrangement in the photosynthetic bacteria (Spoyalov et al., 1996). This H-bonding serves presumably as a conduit for the magnetic interaction between Q_A^- and the iron.

E. On the Role of the Iron

The iron is located midway between the two quinones, but its direct participation in the electron transfer reactions has not been demonstrated. Actually, the use in the iron-quinone complex of a type of iron that is not generally employed in electron transfer reactions, but rather in catalytic reactions, suggests that the iron could serve alternate roles. It cannot be a mere coincidence that PS II, a photochemical center that performs one of the most crucial and at the same time potentially harmful (through its byproducts) reactions (the splitting of water), would employ a reactive and redox active conformation of this type of iron. Of the rather extensive list of proposed roles of the iron (reviewed in Diner and Petrouleas, 1987b; Diner et al., 1991), we will concentrate on a few likely functions.

A minimal role. The similar organization and function of the acceptor side of the reaction centers of the bacteria and PS II, despite the gross differences in the donor side organization and function, suggests that the iron plays an essential role common to both systems. It is reasonably assumed that the iron is an important structural element around which the reaction center is organized (Diner et al., 1991). Furthermore, the role of the iron in stabilizing the semiquinone form of Q_A has been demonstrated (Dutton et al., 1978).

Regulation of the electron transfer rate on the acceptor side. The lability of the iron ligands in non-heme

(non-iron-sulfur) proteins is associated with specific catalytic reactions. In PS II this property is associated with at least one function, the unusual regulation of the electron transfer rate known as the bicarbonate effect. The presence of bicarbonate as a ligand to the iron is essential for the undiminished electron flow between the two quinones. The physiological need for such a control mechanism has been stressed earlier (Diner et al., 1991), and can be outlined briefly as follows. In cases of low CO_2/HCO_3^- stromal concentrations, bicarbonate would dissociate from the iron resulting in a diminished electron transfer rate by PS II and accordingly lower O_2 production, reducing the wasteful reaction of RuBP with excess O_2 (photorespiration). An attractive extension of this idea has considered glycolate, a product of photorespiration and an efficient competitor of bicarbonate, as being involved in a feedback mechanism under these conditions (Petrouleas et al., 1994). It has been noted however, that the binding of glycolate is poor at the physiological high pH of the stromal side. The possibility however, that the relative affinity of bicarbonate and glycolate for the iron site changes during illumination, remains to be tested. Of interest in this respect are the recent experiments with NO implying that the binding affinity of bicarbonate is significantly reduced in the Q_A^- state (Goussias et al., 2002).

Protective functions. The function of the iron-quinone complex in a potentially O_2-rich environment renders it susceptible to damage by the reaction with active oxygen species. Such species could be produced at the donor side or via interaction of O_2 with the reduced quinones (Cleland and Grace, 1999; Nugent, 2001). The iron has accordingly been proposed to have a protective role, acting as an oxidase or a catalase (Diner and Petrouleas, 1987b) or as a weak superoxide dismutase (Nugent, 2001). From a different perspective, the binding of superoxide to a metal center, most likely the non-heme iron, to form a peroxide intermediate has been proposed recently as an important pathway in $OH^{\bullet}$ production during photodamage (Pospisil et al., 2004). It is notable that the iron has all the properties that could support a catalytic role. It has labile ligands, it is redox active, has direct access to the electron transfer chain (Q_A^- reduces Fe^{3+} with a $t_{½} = 7$ μs at pH 6.5, reviewed in Diner and Petrouleas, 1987b), and is properly located between the two quinones.

In summary, while the iron both in BRC and PS II, is an essential structural element of the electron-transport chain, it serves in PS II additional control and protective catalytic roles. It is notable that the location of the iron would couple a catalytic function to photochemical electron transfer. This is a rare combination not found in other proteins employing this type of iron.

III. Organization of the Quinone Binding Sites: The Two-Electron Gate

A. Structural Models of the Quinone Sites

Neither of the earlier crystallographic structures of PS II available at the time of writing (Zouni et al., 2001 (PDB ID 1fe1); Kamiya and Shen, 2003 (PDB ID 1izl)) was at a resolution that allowed detailed discussion, and neither showed a Q_B-site occupant (Chapter 18 and 19). This likely reflected both a weaker occupancy of the Q_B-site than of the Q_A-site, and also some loss of structural integrity on detergent extraction, so that the isolated protein had an even lower occupancy than in situ. Based on the homology in sequence between D1, D2, and L, M subunit pairs, and the common physicochemical and biochemical properties of the acceptor side, several groups had modeled structures for the PS II site, using the reaction centers from *Rps. viridis* and *Rb. sphaeroides* as a template (Crofts et al., 1987; Bowyer et al., 1990; Ruffle et al., 1992; Xiong et al., 1998a). For the Q_A-site, much spectroscopic evidence is available to support the validity of these models, as discussed above, but no detailed spectroscopic information of a similar quality is available for the Q_B site. As a consequence, discussion of the structure-function interface has had to depend on indirect methods for information about the molecular architecture. The BRC-based models served as a valuable aid for understanding the binding of plastoquinone and inhibitors to the Q_B-site of Photosystem II, and although the earlier Photosystem II structures were at a relatively low resolution, they did show a conformation around the putative Q_B pocket similar to that expected from the models. Since submission of this review, a more complete structure has become available (Ferreira et al., 2004; PDB ID 1s5l) that contains both Q_A and Q_B quinones (Fig. 1), and in which side chain coordinates have been modeled. The structure shows a configuration of the acceptor side similar in essentials to that modeled in the late 1980s (Crofts et al., 1987) (Fig. 2), although rotamers chosen for side chains in the earlier model were in some cases

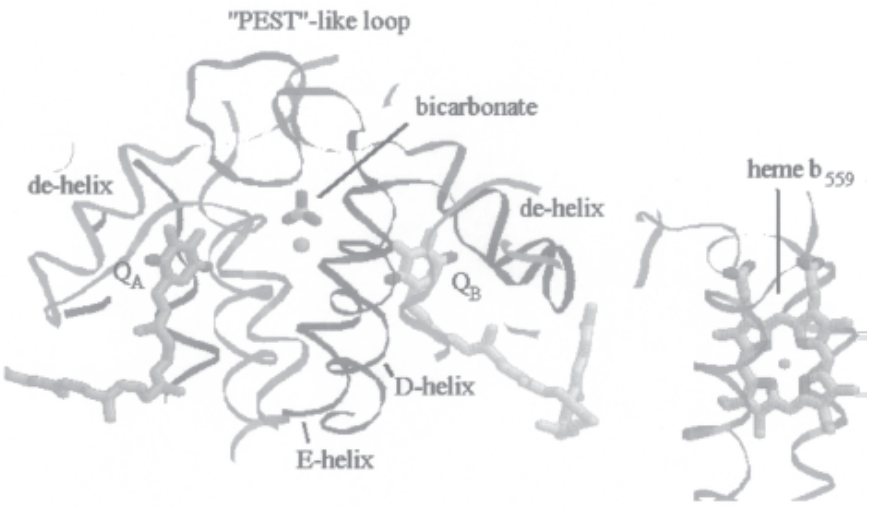

Fig. 1. Photosystem II viewed from the side to show the topology of the acceptor side. Coordinates were taken from the structure by Ferreira et al. (2004) (PDB ID 1s5l), by abstraction of a monomer of the main functional subunits and chromophores. The D1 subunit is in blue (with the 'PEST'-like loop in magenta), D2 in green, shown by ribbons. Prosthetic groups are shown as stick models, with C-atoms of Q_A in orange, Q_B in yellow, and bicarbonate and heme b_{559} in gray, other atoms in CPK-colors. Other structural features discussed in the text are indicated. **See Color Plate XX. [Author, please provide new legend for B&W version]**

inappropriate. The configuration consists of the C-terminal end of the **D**-helix, followed by a loop (the 'PEST'-like loop, with no homology in the bacterial structure) connecting to a transverse helix **de**, which is connected by a sharp turn and an extended loop to the N-terminal end of helix **E**. These spans frame the Q_B binding pocket. The helical ends of **D** and **E** were expected to contain the conserved Fe ligands, D1-His 215 and D1-His272, now identified as such in the Ferreira et al. (2004) structure.

In BRCs, the H-bonding of the quinone at the Q_B-site, and the mechanistic implications, are still somewhat controversial. Interpretation of earlier structures was likely confused by partial occupancy, and by contributions to the electron densities from water, and from quinone in two different positions (Stowell et al., 1997; Lancaster and Michel, 1997). In more recent studies with *Rb. sphaeroides*, structures of the dark-adapted reaction center show most of the quinone displaced about 5 Å out of the pocket (Stowell et al., 1997; Fritzsch et al., 1998; Kuglstatter et al., 2001). On illumination, the quinone rotates and moves so that the Q_B-pocket is fully occupied, likely by a reduced form (Stowell et al., 1997). The functional significance of the quinone displacement seen in these crystallographic structures has been challenged by Breton and colleagues on the basis if FTIR spectra that favor a proximal position for the active quinone, similar to that observed for the semiquinone (Breton et al., 2002; Nabedryk et al., 2003). Studies of the temperature dependence of electron transfer from Q_A^- to Q_B in spinach chloroplasts, combined with measurements of protein flexibility through Mossbauer spectroscopy of ^{57}Fe-enriched material have shown an inhibition that correlates with decreased flexibility (Reifarth and Renger, 1998; Garbers et al., 1998). This was interpreted as showing a similar need for structural reorientation of the headgroup of plastoquinone in the Q_B-pocket of PS II. However, in view of the FTIR evidence, this interpretation should be regarded as tentative. In the BRC, the bonding of the reduced form after illumination was similar to that originally suggested in the *Rps. viridis* structures (1prc and 2prc; Deisenhofer et al., 1995; Lancaster and Michel, 1999), including H-bonds with the L-subunit to His190 (an Fe-ligand), backbone -NH groups from Ile224 and Gly225, and to -OH of Ser223. The latter was also H-bonded to Asn(Asp)213. When ubiquinone is displaced by 1,3,5-triazine (7prc), the herbicide binds through similar H-bonds to the two backbone -NH groups and to –OH of Ser223 and also to –OH of Tyr222 (Lancaster and Michel, 1999). The H-bonding distances suggest that the serine bond is no stronger with triazine (2.93 Å) than with the UQ-2 (2.79 Å).

In BRCs, extensive kinetic, mutational and com-

Note on figures: The hard copy figures provided were not very high quality and were printed on ordinary copier paper. The result is that they are not very sharp.

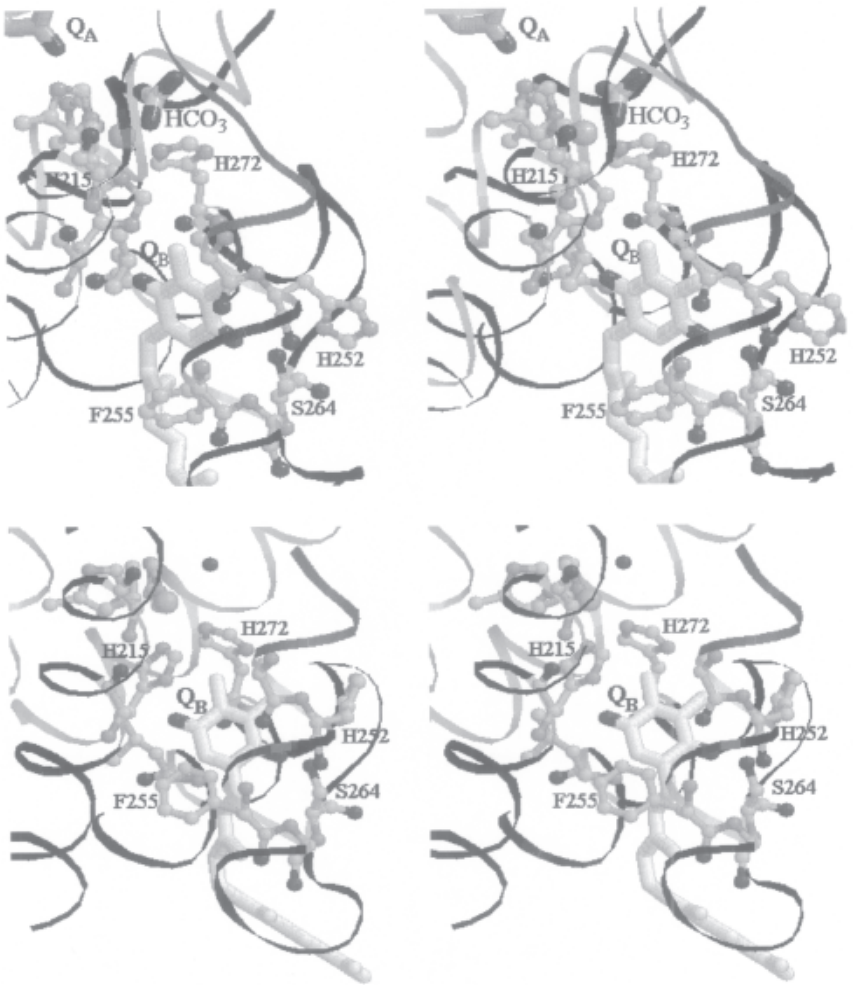

Fig. 2. The Q_B-site structure compared to the model. The structure is from PDB ID 1s5l (Ferriera et al., 2004) viewed looking down into the Q_B-site from the N-phase. The model is that from Crofts et al. (1987), with refinement by H. H. Robinson, Yerkes and A. R. Crofts (unpublished) viewed from a similar perspective. Residues referred to in the text are highlighted.

putational studies have provided a comprehensive picture of the mechanism of electron and proton transfer (reviewed by Okamura et al., 2000; Wraight, 2004), but in the structural context of the proteolipid/detergent micelle. In PS II, kinetic characterization of mutant strains modified in the D1 subunit, and comparison of the patterns of inhibitor sensitivity, provided some validation of the structural models, as will be discussed at greater length below. In an early model of the PS II Q_B-pocket based on the *Rps. viridis* structure as a template (Fig. 2), we assumed that plastoquinone and atrazine bound to the residues of the D1-subunit shown by alignment to be homologous to L-subunit residues, e.g., His215 (*His190*), Asn266 (*Gly225*), and possibly Ser264 (*Ser223*) (bacterial residues in italics), through H-bonds in the Q_B-site (*A. hybridus* sequence), with additional groups of interest His252 (*Asp (Asn)213*), Phe265 (*Phe216*) (Crofts et al., 1987). The choice of -NH backbone H-bonds was somewhat arbitrary, since, although the putative serine ligand (Ser264/*Ser223*) is well conserved, D1 has an extra residue between Ser264 and His272 (the other Fe ligand) compared to the L-subunit. The figure shows the putative liganding residues, several others modified in strains with herbicide resistance (see below), and His252, suggested to be the residue responsible for binding a proton to stabilize Q_B^- in the site (Crofts et al., 1987; Bowyer et al., 1990). More recent models had suggested additional features that are absent from the bacterial template, including

potential sites for bicarbonate binding (Ruffle et al., 1992; Xiong et al., 1998a). The bi-dentate liganding of the Fe by bicarbonate suggested in the latter model is well supported by EPR and FTIR studies. These features are now all confirmed in the Ferreira et al. (2004) structure.

B. Mechanism of the Two-Electron Gate

1. Kinetic Models of the Two-Electron Gate

Although the Q_B-site has been recalcitrant to exploration by molecular spectroscopy, a major advantage of studies of the two-electron gate in oxygenic systems has been the ability to follow the kinetics of electron transfer in intact membrane preparations through use of the change in fluorescence yield. As the closed reaction center reopens, the high fluorescence yield associated with reduction of Q_A^- evolves to a low fluorescence state with kinetics reflecting the electron transfer to the Q_B-site occupant (Joliot, 1974; Bowes and Crofts, 1980). Because the reaction center communicates with the plastoquinone pool in the native configuration, the rates measured depend not only on the rate constants for electron transfer, but also on the occupant of the Q_B-site (quinone or semiquinone), and on the kinetics of exchange of Q and QH_2 with the pool. Recognition of the contribution of these exchange processes to the kinetics made it possible to obtain detailed kinetic parameters describing both the electron transfer and the interaction with the quinone pool (Robinson and Crofts, 1983).

The commonly accepted model is the two-electron gate proposed by Velthyus (1981) for PS II, and by Wraight (1981) for BRCs, in which quinone and quinol forms freely exchange at the Q_B-site, and the semiquinone form generated after one flash is non-exchangeable. However, we should note that there are dissenting views (Kashino et al., 1996). Kinetic models for the reactions of the two-electron gate in BRCs and chloroplasts have been extensively reviewed (Crofts and Wraight, 1983; Shinkarev and Wraight, 1993; Okamura et al., 2000; Wraight, 2004).

In an early model for green plants, based on experiments with pea thylakoid membranes, Robinson and Crofts (1983) recognized explicitly the relatively weak binding of plastoquinone, required to account for the biphasic nature of the electron transfer following a single flash from the dark-adapted state. The slower phase was attributed to the second-order process of reduction of quinone from the pool (Scheme 2). A similar model has recently been used to measure the deuterium isotope effect on the rates of the separate electron transfers (de Wijn and van Gorkom, 2001). In the earlier model, the pH dependence of the apparent equilibrium constant for sharing an electron between primary and secondary quinones, K_{app}, was accounted for by postulating a single residue close to the Q_B-site whose pK was changed when Q_B was reduced to form the semiquinone anion (Robinson and Crofts,

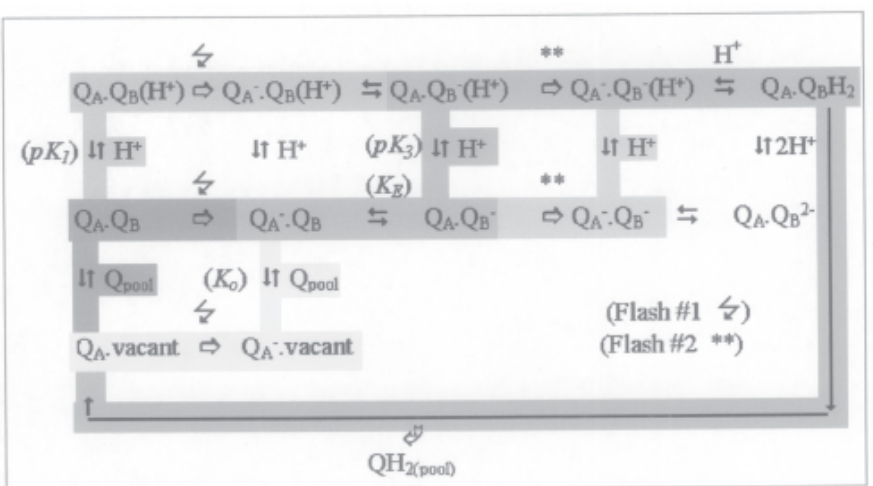

Scheme 2. The kinetic model discussed. Under physiological conditions, most centers start in the blue box, and progress through the green path. The remainder start in the yellow box, and rejoin the green pathway after the second-order binding of Q from the pool. See text for details.

Please provide a new legend for this B&W figure. Also, is this going to be one of the Color Plates? As before, the hard copy of this is not very good and will not reproduce well.

1983, 1987; Crofts et al., 1984). With modification, this model also accounted well for the kinetics and thermodynamics of inhibitor binding at the Q_B-site (Taoka and Crofts, 1987; Taoka, 1989), of electron transfer in susceptible and resistant *Amaranthus hybridus* biotypes (Bowes et al., 1980; Taoka, 1989; Taoka and Crofts, 1990), and in herbicide resistant mutants of *C. reinhardtii* (Crofts et al., 1993). Since this more complete model has been described only briefly (Taoka and Crofts, 1990), we will summarize its main points here.

The biphasic kinetics in the 10 ms range were assumed to reflect two distinct populations of PS II. Reaction centers after long dark adaptation have either a secondary quinone bound at the Q_B-site (Q_AQ_B), or a vacant Q_B-site (Q_A.vacant), as shown in Scheme 2. An actinic flash produces either Q_A^-.vacant, or $Q_A^-Q_B$. Both Q_A^-.vacant and $Q_A^-Q_B$ are closed centers, with the same high fluorescence yield. At time >50 μs after the flash, when reactions on the donor side have reached equilibrium, the fluorescence yield reflects the electrons remaining on Q_A^-. In centers initially in the Q_AQ_B state, the electron is transferred to Q_B in a first-order process, generating $Q_AQ_B^-$ (with low fluorescence), with a half time of approximately 150 to 200 μs. Since the electron on Q_A can be transferred to Q_B only when a plastoquinone is present at the Q_B-site, electron transfer in centers initially with a vacant site must first involve a binding of quinone in a second-order process, and then transfer of the electron, with a slower kinetics reflecting the convolution of the binding and electron transfer reactions. Both phases are well fitted by exponential decay curves. Since the more rapid phase accounted for more than half those centers which transfer an electron within 10 ms, and the quinone pool was oxidized under our conditions, the minor fraction of initially vacant centers would become occupied from a pool of plastoquinone in > five-fold excess over the reaction center. Reaction from this pool would therefore follow pseudo-first-order kinetics.

Rate constants for electron transfer and binding reactions can be calculated from the kinetic curves for the two separate electron transfers observed after one or two actinic flashes given to preparations starting in a defined initial state (usually with all centers having an oxidized Q_B, following prolonged dark-adaptation). Analysis of the decay kinetics after the first flash can be greatly simplified by making use of the following explicit assumptions derived from the model outlined above: (*i*) the ratio of the amplitude of the fast component to that of the slow component in the decay kinetics following an actinic flash is equal to the ratio of the fraction of reaction centers initially in the Q_AQ_B state over that in the Q_A.vacant state; (*ii*) under our experimental conditions, the binding of a plastoquinone to the vacant site is a pseudo-first order reaction; (iii) the dissociation constant of a plastoquinone from its binding site following an actinic flash (from $Q_A^-Q_B$) is the same as that in the dark (from Q_AQ_B).

Solution of the standard rate equations gives Eqs. (1) and (2) for the observed rate constant r_1 and r_2. The apparent equilibrium constant for sharing an electron between quinones Q_A and Q_B is K_{app}, defined in Eq. (3). The dissociation constant, K_0, of plastoquinone from the Q_B-site, is the ratio of the on- and off-rate constants (k_{AV}, k_{VA}) (Eq. (4)). K_E is the equilibrium constant for the electron transfer reaction, with forward and reverse rate constants k_{AB} and k_{BA}. The equilibrium constants are related through Eqs. (3) and (4) (see below for further discussion).

$$r_1 + r_2 = k_{VA}(1 + K_0) + k_{BA}\{1 + K_{app}(1 + K_0)\} \quad (1)$$

$$r_1 r_2 = k_{VA} k_{BA}(1 + K_0)\,(1 + K_0) \quad (2)$$

$$K_{app} = \frac{[Q_A Q_B]}{[Q_A^- \cdot vac] + [Q_A^- \cdot Q_B]} = \frac{\frac{k_{AB}}{k_{BA}}}{\left(1 + \frac{A_0}{B_0}\right)} = \frac{K_E}{(1 + K_0)} \quad (3)$$

$$K_0 = \frac{A_0}{B_0} = \frac{k_{AV}}{k_{VA}} = \frac{[Q_A \cdot vac]}{[Q_A Q_B]} \quad (4)$$

In these equations, species in square brackets represent fractions of the reaction centers in a particular state as indicated in the bracket. States $Q_A.vac$ and $Q_A^-.vac$ represent centers with a vacant Q_B-site, with the Q_A oxidized and reduced respectively. Variables r_1 and r_2 are the measured rate constants for the slow and fast phases of electron transfer derived directly from the biphasic decay kinetics of Q_A^- by fitting the kinetic curves with two exponential components and a residual. The Q_A^- kinetics are obtained from the fluorescence curves after the latter have been corrected for the non-linear relation between fluorescence yield and concentration of Q_A^-. Variables A_0 and B_0 are the amplitudes of the slow and fast components of the

Table 1. Physico-chemical constants for the reactions of the two-electron gate following an actinic flash

Constant	Reaction	wild type	S264G	notes
A. pK values				(1)
pK_1 Q_AQ_B (H^+)	$\leftrightarrows Q_AQ_B + H^+$	6.2	6.2	
pK_2 Q_A.vac (H^+)	$\leftrightarrows Q_A$.vac + H^+	6.9	6.2	
pK_3 $Q_AQ_B^-$ (H^+)	$\leftrightarrows Q_AQ_B^- + H^+$	8.1	7.0	
B. Equilibrium (K) or rate (k) constants				
$K_{O, pK}$	$Q_A^-Q_B \leftrightarrows Q_A^-$ (+ Q_{pool})	0.12 ± 0.02	0.57 ± 0.06	(2,3)
K_E	$Q_A^-Q_B \leftrightarrows Q_AQ_B^-$	3.1 ± 0.7	4.7 ± 0.8	
k_{VA}	Q_A^- (+ Q_{pool}) → $Q_A^-Q_B$	500	650	(2,4)
k'_{VA}	$Q_A^-(H^+)$ (+ Q_{pool}) → $Q_A^-Q_B(H^+)$	500	650	(2,4)
k_{AV}	$Q_A^-Q_B$ → Q_A^- (+ Q_{pool})	60	370	(2,4)
k'_{AV}	$Q_A^-Q_B(H^+)$ → Q_A^-(H^+)(+ Q_{pool})	300	3,370	(2,4)
k_{AB}	$Q_A^-Q_B \uparrow Q_AQ_B^-$	3,000	10,000	(5,6)
k'_{AB}	$Q_A^-Q_B(H^+)$ → $Q_AQ_B^-$(H^+)	3,000	10,000	(5,6)
k_{BA}	$Q_AQ_B^-$ → $Q_A^-Q_B$	987	2,200	(5,6)
k'_{BA}	$Q_AQ_B^-(H^+)$ → $Q_A^-Q_B(H^+)$	12	340	(5,6)

Notes. (1) It is assumed that values for pK_1 and pK_2, and the fraction of vacant reaction centers in the dark (determined by K_O), are the same after dark adaptation as those following an actinic flash. (2) Although these reactions involve the quinone pool, constants shown are based on the pseudo-first-order process, with $[Q_{pool}]$ assumed to be 1. (3) The true value can be obtained from $K'_O = K_O [PQ]_{pool}$; we have previously estimated $[PQ]_{pool}$ = 5 mM under oxidizing conditions (Crofts et al., 1984). (4) Rate constants k_{ij} are for reaction at pH above pK_2. Rate constants k'_{ij} are for reaction at pH below pK_1. (5) Rate constants k_{ij} are for reaction at pH above pK_3. Rate constants k'_{ij} are for reaction at pH below pK_1. (6) The difference between rate constants k and k′ does not reflect a change in the rate constant for the electron transfer process (since K_E is independent of pH), but a change in concentration of substrate for the backreaction, $[Q_AQ_B^-]$, associated with pK_3.

biphasic decay kinetics, again obtained directly from kinetic analysis of the data.

Using the above equations, the four rate-constants k_{AV}, k_{VA}, k_{AB} and k_{BA} (defined in Table 1) can be determined from four measured parameters; the fast and slow apparent rate constants; the fraction of vacant (or Q_B-bound) reaction centers (both determined from the corrected decay kinetics); and the apparent equilibrium constant, K_{app}. This last variable is the only term not obtained directly from the kinetic experiments. In fluorescence experiments, it can be measured from the ratio of back-reactions from Q_A^- or from $Q_AQ_B^-$. The former can be measured from the decay of Q_A^-, measured through fluorescence yield, or spectrophotometry, following illumination by a saturating flash in the presence of DCMU; the latter from loss of the binary pattern when the fluorescence yield decay was monitored at ~200 μs following a series of flashes (Robinson and Crofts, 1983, 1987), or through the $S_2 \rightarrow S_1$ deactivation on the donor side. The equilibrium constant can also be determined through thermoluminescence from the temperatures for Q and B components (Rutherford et al., 1982).

Another feature of importance in fitting theoretical curves to the experimental results was the fraction of centers in which the decay of fluorescence occurs in the seconds time range, attributed to non-functional centers. This fraction was often higher in mutant strains than in the native strain, but we do not have a ready explanation for this in the framework of our model. Inhomogeneities in the population of PS II that give rise to differences in kinetic behavior as assayed by fluorescence have been discussed extensively elsewhere (Govindjee, 1990; Joliot et al., 1992; Lavergne et al., 1992), and are outside the scope of this review.

2. The pH Dependence of the Apparent Equilibrium Constant, K_{app}

Measurement of K_{app} as a function of pH showed a dependence over the range 5.5–8.0, indicating that the

$Q_AQ_B^-$ state was stabilized by uptake of a H^+ (Robinson and Crofts, 1984). The curve could be well fit by assuming that a single group underwent a pK change from ~6 (pK_1) to ~8 (pK_3) due to the Coulombic effect experienced by the group on formation of a semiquinone anion on reduction of Q_B. Similar studies of the pH dependence of rate and equilibrium constants in a herbicide resistant strain of *A. hybridus* showed that the pH dependence changed on mutation of D1-Ser264 to glycine (Taoka and Crofts, 1990; Crofts et al., 1993). Part of the change could be attributed to a change in K_0; in the wild biotype, the fraction of the reaction centers with a vacant Q_B-site was found to vary with pH, but this dependence was lost in the mutant strain. The pH dependence for binding could be characterized by two pKs, given in Eq. (5).

$$K_0 = \frac{[Q_A \cdot vac]_{tot}}{[Q_AQ_B]_{tot}} = \frac{[Q_A \cdot vac] + [Q_A \cdot vac(H^+)]}{[Q_AQ_B] + [Q_AQ_B(H^+)]} = \frac{[Q_A \cdot vac]_{pK_2}}{[Q_AQ_B]_{pK_1}} \frac{\left(1 + \frac{[H^+]}{K_2^d}\right)}{\left(1 + \frac{[H^+]}{K_1^d}\right)} \quad (5)$$

where K_0 is the value of the dissociation constant measured at a particular value of pH. The terms $[Q_A.vac]_{pK}$ and $[Q_AQ_B]_{pK}$ are the fractional concentrations of vacant and Q_B occupied centers at pH above pK_2 (assumed to be the higher pK value), and K^d_1 and K^d_2 are the acid dissociation constants of $Q_AQ_B(H^+)$ and $Q_A.vac(H^+)$, respectively. With the simplifying assumptions given above, Eq. (5) expresses the pH dependence of K_0 and hence of A_O/B_O (Eq. (4)). The factor $[Q_A.vac]_{pK}/[Q_AQ_B]_{pK}$ gives $K_{0,pK}$, the dissociation constant above pK_2. The results (summarized in Table 1) show that in the physiological range, plastoquinone binds more tightly at the Q_B-site in the susceptible than in the resistant strain. This raises interesting mechanistic questions to be discussed further below.

3. Estimation of the Rate Constants for the Reactions Including the Protonated Species, and Proton-Uptake at the Q_B-site

The rate constants for reactions involving both protonated and unprotonated species can be calculated from three pKs and the rate constants obtained from kinetic experiments. The parameters can be expressed in terms of these pKs, and following the same rationale as above, the following equations can be used in analysis of the kinetic data:

$$K_{app} = \frac{K_E}{(1+K_0)} \frac{\left(1 + \frac{[H^+]}{K_3}\right)}{\left(1 + \frac{[H^+]}{K_1}\right)}$$

from which

$$\frac{k_{AB}}{k_{BA}} = K_E \frac{\left(1 + \frac{[H^+]}{K_3}\right)}{\left(1 + \frac{[H^+]}{K_1}\right)}$$

Parameters for K_0 can be obtained through Eq. (5).

Table 1 compares values obtained with susceptible and resistant biotypes. The values of the on-rate constants for quinone binding were similar for both biotypes, in the range from 500 to 650 s^{-1}, and in each case were pH independent. In the resistant biotype, the rate constants for unbinding of quinone were the same from the protonated and deprotonated sites. In the susceptible biotype, the off-rate constant at pH values above pK_2 (i.e. from the deprotonated site) is 6 times smaller than in the resistant strain, and about 5 times smaller than that from the protonated site. As a consequence, in the pH range above pK_2 (the likely physiological range) the susceptible strain binds quinone about 4-5 times more strongly than the resistant strain; in the susceptible strain, a quinone can reach both the protonated and the deprotonated binding species at the same frequency, but it leaves the protonated site 5 times more frequently than the deprotonated site. Below pK_1, both strains show about the same affinity for quinone.

Direct measurement of the kinetics of the two-electron gate from the proton uptake associated with the reduction of the Q_B species in chloroplasts is complicated by a number of problems: (*i*) delays due to exchange with buffering groups in the membrane, and the tortuous pathway through the appressed regions of the grana stacks to the bulk phase (Polle and Junge, 1986); and (*ii*) the indirect coupling

through protonation of protein side-chains, which leads to uptake of a proton on each flash, although the semiquinone is anionic (Fowler, 1977; Saphon and Crofts, 1977; Hope and Morland, 1979; Hope and Matthews, 1983; Robinson and Crofts, 1984; Crofts et al, 1987). Detailed discussion of these difficulties is beyond the scope of this review, but the interested reader is referred to a paper by Haumann and Junge (1994), who measured rates corresponding more closely to the electron transfer rates by using neutral red (NR) as an indicator. Interestingly, the proton uptake was slower on the first flash (760 μs for H^+-uptake compared to150 μs for the electron transfer) than on the second flash (300 μs compared to 620 μs for the electron transfer). This was interpreted as showing that transfer of the second electron depended on protonation of the $Q_A^-Q_B^-$ state, as suggested in bacterial reaction centers (Wraight, 1979).

4. The Second Order Rate Constant for Binding of Plastoquinone

The turn-over time of the two-electron gate can be measured from the reduction of the plastoquinone pool on strong illumination, which takes about 20 ms (Stiehl and Witt, 1968). With about 10 quinone molecules/PS II in the pool, this represents about 2 ms for the transfer of each pair of electrons, including all binding and unbinding reactions. A similar value was found from the rate of generation of the species able to accept a proton, with half time of 0.8 ms (Hope and Matthews, 1983). In experiments in which the reopening time was studied by varying the delay time between the second and third flashes of a series, the Q_B-site was able to evolve from the $Q_A^-Q_B^-$ state, formed immediately after a second flash from the dark-adapted state, to Q_AQ_B state, detected by the characteristic rapid kinetics, with half time of 0.6 ms (Robinson and Crofts, 1987). The overall process involved electron transfer, unbinding of QH_2 and binding of Q, so the observed halftime must reflect a convolution of times for these partial processes, each of which was less. The pseudo-first order rate constants for binding of quinone derived from the kinetics after the first flash (k_{VA}) involved only a fraction of centers - those with a vacant binding site. When adjusted to compensate for this fraction, the approximate half times for binding of quinone are 0.4 and 0.8 ms for the susceptible and the resistant biotype, respectively, in good agreement with earlier values. The second-order rate constant for the binding of quinone can be found by using these values and an estimated concentration for plastoquinone in the membrane. Assuming these to be 5 mM in the susceptible and 4 mM in the resistant strains, the second order rate constants (referred to concentrations in the membrane) are found to be $1 \times 10^5\ M^{-1}s^{-1}$ and $2 \times 10^5\ M^{-1}s^{-1}$, respectively. The dissociation constant for plastoquinone with respect to membrane concentration, $K'_0 = K_0[Q_{pool}]$, is then 0.6×10^{-3} M in the susceptible and 2.28×10^{-3} M in the resistant strain (see Table 1, and legend).

5. The Pathway for Electron Transfer in Susceptible and Resistant Biotypes

In the physiological pH range (e.g. pH 7–8), the distribution of states is rather different in the susceptible and resistant biotypes, so that the pathway for electron transfer shows different characteristics. In the susceptible strain, most centers (80-90%) have the Q_B-site occupied, and electron transfer occurs from $Q_A^-Q_B$ with the forward rate constant of $3 \times 10^3\ s^{-1}$, and terminates either on $Q_AQ_B^-$ (with 20%) or on $Q_AQ_B^-(H^+)$ (with 80%). In the resistant biotype, only about two thirds of the Q_B-sites are initially occupied; in these centers, electron transfer occurs from $Q_A^-Q_B$ with the rate constant of $10^4\ s^{-1}$; in the remaining centers, electron transfer occurs through the second-order route following binding of plastoquinone. The reaction comes to equilibrium with a substantial fraction of centers still in the Q_A^- state; of those centers undergoing successful forward electron transfer, the electron was distributed with ⅔ on $Q_AQ_B^-$ and ⅓ on $Q_AQ_B^-(H^+)$.

6. Role of D1-Ser264 in the Mechanism of the Q_B-Site

The mechanism discussed above was developed in the context of experiments with wild-type and herbicide resistant strains of *A. hybridis*. The resistant strain followed the general trend for atrazine tolerant mutants of higher plants where Ser264 is replaced by glycine (Hirschberg and McIntosh, 1983; Goloubinoff et al., 1984; Bettini et al., 1987; Taoka and Crofts, 1990; Sunby et al., 1993). In contrast, in *C. reinhardtii* (Erickson et al., 1984) and cyanobacteria (Golden and Haselkorn, 1985; Ajlani et al., 1989a, b) the common substitution is by alanine. More recently, a resistant mutant of *Euglena* was described that carries a substitution of the homologous Ser265 to

threonine (Aiach et al., 1992). This repeated loss of Ser264 is highly significant, indicating that it might play an important role in herbicide binding. Trebst (1986) and Bowyer and co-workers (1991) suggested that Ser264 contributes to the binding of inhibitors of the urea-atrazine family to the Q_B site by H-bonding of its side chain hydroxyl group to the NH group in the herbicide molecule, in analogy with the observed H-bonding of the herbicide terbutryne to Ser223 in the L subunit of bacterial reaction centers (Michel et al., 1986). Another study (Tietjen et al., 1991) proposed that Ser264 would stabilize the structure of the Q_B site by H-bonding to His252. This histidine residue could also be involved in binding of the proton that stabilizes the semiquinone Q_B^- in the pocket (Crofts et al., 1987).

The change of Ser264 to glycine in the resistant strain was associated with a change in affinity for atrazine of about 3300-fold, but of only about 10-fold for plastoquinone. The resistivity for atrazine represents a change in binding free-energy of 20.3 kJ.mol^{-1}, in the range expected for a buried H-bond, but for plastoquinone, the 10-fold change in binding represents only 5.65 kJ.mol^{-1}. The differential change in affinity may be understood in terms of the model discussed above if one or both of the two back-bone H-bonds are ligands for plastoquinone, but the serine -OH forms only a weak H-bond. Conversely, the serine -OH forms a strong H-bond for the herbicide.

Perhaps the most intriguing aspect of the studies of Taoka and Crofts (1990) was that the mechanistic phenotype of the resistant strain differed from the susceptible strain through pK changes. Since serine does not have a pK in the physiological range, this suggests that the loss of Ser264 involves also a loss of interaction with a dissociable group. In our sequence alignment, His252 occupied the same position relative to a conserved phenylalanine (255 in D1, 216 in *Rps. viridis* L-subunit) as L-Asn(Asp)213 in the BRCs, and was naturally positioned in the model to form a H-bonded with Ser264. These interactions might facilitate a proton relay mechanism by which proton(s) could be transferred to the Q_B-site on reduction by a second electron. The results could then be explained by a fractional contribution of the Ser264 -OH to quinone binding, modulated by a sharing of the H-bond with His252. The structural speculations underlying this mechanistic model have been validated by the Ferreria et al. (2004) structure, and these authors also suggested a similar involvement of His252 in interactions with Ser 264 in stabilization of the SQ. Details of the functional relation of the structure to the pKs identified in this work remain to be determined. However, results from mutagenesis of His252 in *C. reinhardtii* (Padden S and Crofts A, unpublished, and see below) support a model of this sort.

C. Binding of Inhibitors and Exogenous Quinones at the Q_B-Site

The studies summarized above have strongly suggested that Q_B is relatively weakly bound. This is also apparent from the ease with which it can be displaced by exogenous electron acceptors and various inhibitors (Velthuys, 1976; Bowes and Crofts, 1981a; Velthuys, 1982; Lavergne, 1982a; Taoka et al., 1983; Crofts and Wraight, 1983; Bowyer et al., 1991). This occurs in several steps, involving electron transfer back to Q_A followed by dissociation of quinone, to generate an intermediate Q_A^-.vacant state that is the substrate for binding. In the case of inhibitor binding, the result is an inhibitor-induced reduction involving the reactions:

$$Q_AQ_B^- \leftrightarrows Q_A^-Q_B \leftrightarrows Q_A^-\{\text{vacant}\} \xleftrightarrow{\text{Inhibitor}} Q_A^-\text{Inhibitor}$$

Exogenous quinones can follow a similar reaction path, with an additional step of electron transfer from Q_A^-, to generate a foreign semiquinone at the site (Lavergne, 1982b; Taoka et al., 1983; Zimmermann and Rutherford, 1986; Petrouleas and Diner, 1987). The mechanism of loss of the Q_B^- species is thought to involve displacement of the oxidized form (Q_B) present in a fraction of centers as a result of the relatively small equilibrium constant favoring electron transfer from $Q_A^-Q_B$ to $Q_AQ_B^-$. If the exogenous reagent is an electron acceptor (for example, benzoquinone), the semiquinone is generated. If the semiquinone has a high enough potential, it can accept an electron from the non-heme Fe, to generate the oxidized form:

$$Q_A.Fe.Q_B^- \leftrightarrows Q_A^-.Fe.Q_B \leftrightarrows Q_A^-\{\text{vacant}\} \xleftrightarrow{Q_{ex}}$$
$$Q_A.Fe.Q_{ex}^- \leftrightarrows Q_A.Fe^+.Q_{ex}^{2-}$$

A consequence of the reaction pathway leading to inhibitor-induced reduction of Q_A is that the titer of inhibitor is higher for binding to the $Q_AQ_B^-$ state than to the Q_AQ_B state (Lavergne, 1982c; Taoka and Crofts, 1987). A second consequence is that inhibitor binding is pH dependent.

Taoka and Crofts (1987) investigated kinetic aspect of inhibitor binding to the oxidized and 1-electron reduced states of the Q_B-site, and measures on and off rate constants as a function of pH for several different inhibitors (DCMU, atrazine, *o*-phenanthroline, and two cyanoacrylate derivatives 964S and 965, Huppatz and Phillips, 1984, which differ by stereo rotation about one C-atom), as summarized below:

1. Binding of inhibitors to the oxidized state of the secondary quinone site was essentially pH independent.

2. Binding to the one-electron reduced state was slower, and strongly pH dependent.

3. For all the inhibitors studied, both the difference in rate, and the pH dependence, could be accounted for in terms of a simple hypothesis. They reflect the lowered concentration of the open sites at which the inhibitor binds, associated with formation of a stable semiquinone at the site. The concentration of open sites was described by the set of equilibrium constants determining the distribution of an electron between primary and secondary quinone acceptors discussed above.

4. When these factors were accounted for, the second-order rate constants for inhibitor binding were found to be constant with pH, and close to those for binding to oxidized centers, assuming that the reaction partner was the vacant quinone binding site in either state, and that the binding constant for plastoquinone from the pool was the same for oxidized and one-electron reduced centers.

5. Second-order rate constants for binding and unbinding of each of the inhibitors with respect to concentration in the membrane phase were determined by taking account of the partition coefficients between aqueous and membrane phase. DCMU and the two cyanoacrylates showed similar values for binding rate constant ($2–8 \times 10^4\ M^{-1}.s^{-1}$), close to the value estimated for plastoquinone binding ($\sim 10^5\ M^{-1}s^{-1}$, see above), but *o*-phenanthroline was slower (about $0.4 \times 10^4\ M^{-1}.s^{-1}$). DCMU and 964S are effective inhibitors because of their very slow unbinding ($<0.02\ s^{-1}$), but 965R is an ineffective inhibitor because of its rapid unbinding ($2–3\ s^{-1}$). The bulky *o*-phenanthroline is a poor inhibitor both because of its slower rate of binding, and relatively high rate of unbinding ($0.3\ s^{-1}$).

Several of these conclusions are of more general interest to wider studies of binding from the lipid phase, since it is likely that similar sites in other quinone processing enzymes will show similar characteristics. Inhibitor binding follows a pattern familiar from studies of soluble enzymes, except that the relevant concentration term is that for the membrane phase. The conclusions are also of interest with respect to studies of inhibitor binding using the conventional Quantitative Structure Activity Relationship (QSAR) approach (for a comprehensive view, see Huppatz, 1996; and articles in Yoshida et al., 1993), since they indicate clearly the parameters that underlie some of the fitting variables used to quantify differential aspects of inhibitor binding.

D. Structural and Mechanistic Information from Mutagenesis Studies

1. Herbicide Resistant Strains of Chlamydomonas and Cyanobacteria

Herbicide resistance was originally found in higher plants (see Moreland, 1993, for historical review; Draber et al., 1991; Oettmeier, 1992, 1999), and these continue to provide interesting new strains (Alfonso et al., 1996); however, most recent work on herbicide resistance has been in algae or cyanobacteria, which are more amenable to genetic manipulation. Erickson and co-workers (1984, 1989) and Galloway et al. (1984) studied mutations in the D1-subunit in *C. reinhardtii* generated by selection for herbicide resistance, and these have also been investigated in greater detail in other labs (Baroli, 1992; Govindjee et al., 1992; Draber et al., 1993; Crofts et al., 1993; Oettmeier et al, 1993; Tietjen et al., 1993). These studies have covered detailed measurements of inhibitor resistance for a wide range of inhibitors, kinetic analysis, and use of QSAR and computational modeling to predict from the differential inhibitor sensitivities structural features associated with differential binding.

In a detailed kinetic study, following the protocols outlined above, Baroli and colleagues (Baroli, 1993; Crofts et al., 1994) were able to deconvolute the contributions of rate constants and equilibrium constants for plastoquinone binding and electron transfer to the overall process. Two mutations in D1, Ser264Ala and Ala251Val, led to a marked slowing of kinetics for reduction of plastoquinone to the bound semiquinone.

In Ser264Ala, the second electron transfer was also slower, but was normal in Ala251Val. In mutant Gly256Asp, the electron transfer kinetics were normal after the first flash, but slowed after the second. In mutants Leu275Phe, Val219Ile, and Phe255Tyr, the electron transfer kinetics after both flashes were similar to those in wild type. Among the amino acid substitutions in D1 covered by these studies, two clear groups could be established:

1. Mutations that confer herbicide resistance, but had no marked effect on the electron transfer between the plastoquinone acceptors of PS II. These mutations are Val219Ile, Phe255Tyr, Leu275Phe and Gly256Asp (Table 2). In the case of Gly256Asp, the normal kinetic parameters observed were in contrast to a slowed electron transfer reported from earlier work (Erickson et al., 1989; Govindjee et al., 1992). However, the earlier experiments were performed using averaging, with a short dark period between actinic flashes. When the experiment was performed under uncoupled conditions and with a longer dark interval, electron transfer on the first flash was similar to wild type, but that after a second flash was inhibited. It seems likely that the slowed kinetics previously reported reflected a dominant contribution from a mixed population of states, with the inhibited 1-electron reduced state dominating, and possibly some slowing due to reduction of the plastoquinone pool. The slowed electron transfer on the second flash may have reflected an interference of the aspartate side chain with proton processing associated with the second electron transfer.

2. Mutations that confer herbicide resistance and considerably modify the electron transfer between the plastoquinone acceptors, as with Ser264Ala and Ala251Val. In general, the Ser264Ala mutation showed in exaggerated form the characteristics of the Ser264Gly mutation in high plants. Only a slight change in the apparent equilibrium constant for electron transfer was observed. The slow electron transfer in this mutant was due to a high dissociation constant for plastoquinone rather than a change in K_{app}. This supports the suggestion that Ser264, besides being involved in the binding of inhibitors, also plays an important role in plastoquinone binding. The high value of K_0 comes from an increased fraction of centers in the state Q_A.vacant in the dark. Also, both the on- and off- rate constants for binding and dissociation of plastoquinone are increased in this mutant. In centers in the Q_AQ_B state, however, the electron transfer reaction proceeds 3.5 times more rapidly than in wild type. Assuming structural homology with the bacterial reaction center, the loss of the –OH on Ser264 might be expected to result in a weaker binding, or binding to an alternative site, at the end of the pocket distal from the Fe in these mutant strains as discussed above. Since reaction centers are strongly dependent on distance, the more rapid rate for the bound quinone might reflect a shorter bonding distance to the N of D1-His215, which provides a H-bond to the other quinone — C=O at the proximal end of the binding pocket for electron transfer reactions. In effect, the mutations may 'push' the plastoquinone molecules closer together, allowing for a faster electron transfer.

The structural basis for differential inhibitor resistance has been explored in detailed QSAR studies using the mutant strains tested against a wide range of substituted triazines and triazinones (Tietjen et al., 1993) and 4-nitro-6-alhylphenols (Draber et al., 1993). Complementary studies at some of these sites have explored a wider range of mutations (Forster et al., 1997; Lardans et al., 1997; Johanningmeier et al., 2000) that extend the database for discussion of structure-function relationships.

2. Specific Mutagenesis of Herbicide Resistance Sites in Synechocystis

Following earlier work on spontaneous mutants selected for herbicide resistance (Robinson et al., 1987), a similar set of mutants showing various degrees of herbicide resistance have also been generated in *Synechocystis* sp. PCC 6714, both as single mutants, and with combinations of changes at the individual sites (Astier et al., 1986, 1993; Etienne et al., 1990). These showed interesting variations in selectivity for different herbicides compared to the results fro *Chlamydomonas* and higher plants.

3. Combinatorial Mutagenesis of a Conserved Span of the de Loop

Vermaas and colleagues (Vermaas et al., 1989; Kless et al., 1993; Kless and Vermaas, 1995) used combinatorial mutagenesis to explore the role substantial

spans between helices **D** and **E** of D1 and D2. In the Kless et al. (1993) study, spans from the loop starting at the end of helix **D** of D2 were replaced by residues from the equivalent span in D1. Interestingly, the mutant strains retained function with relatively minor changes, but these include changes in herbicide binding or stability of the semiquinones at both sites, as measured from glow curves, indicating perhaps that although the span contributes little to either catalytic site, there are pleotrophic effects over a larger volume. This is in line with the structural data. In the Kless and Vermaas (1995) study, the role of four conserved residues (Tyr254, Phe255, Gly257, Arg257) in the putative **de**-helix of the D1 subunit of the *Synechocystis* sp. PCC 6803 was explored. 25 mutants with functional PS II were isolated, all of which showed different codon combinations at positions 254 to 257. None of the conserved residues was found to be mandatory for PS II function. However, 24 of the functional mutants contained Tyr or Phe at position 254 while at the other three positions many different amino acid combinations could be functionally accommodated. Most of the PS II properties were similar in the mutants compared to wild type. Noticeable modifications in the mutants concerned the semiquinone equilibrium on electron transfer between Q_A and Q_B, and the affinity of PS II inhibitors. The authors concluded that, even though many different combinations of amino acids in positions 254 to 257 may satisfy the primary function, complex requirements need to be combined for optimized performance. Most functional sequences maintained an amphipathic arrangement, assuming a helical conformation. In their alignment, Tyr254 was proposed to be functionally analogous to Phe216 of the L subunit in purple bacteria, and they suggested that Tyr254 faced the Q_B binding pocket to allow a contribution to binding of Q_B. The alternative candidate for the residue functionally equivalent to Phe216 is Phe255, as suggested in the Crofts et al. (1987) model, and this is the configuration shown in the Ferreira et al. (2004) structure. The rotation of the helical axis by ~100° brings the polar face of the helix to the aqueous interface, positioning His252 for interaction with Ser264.

4. Specific Mutagenesis of D1-His252 Shows an Important Role in H^+-Processing

Diner ad co-workers (1991) briefly reported a mutation of His252 in the **de** helix of the Q_B-site (His252Leu) of *C. reinhardtii*, studied in collaboration with Peter Nixon, which showed an inhibited electron transfer to Q_B. Padden and Crofts (unpublished) have constructed a more extensive series of mutants at this site (His252Asp, Lys, Asn and Gln) in order to test the role in stabilization of the semiquinone and proton delivery. Only the His252Asp mutant was able to grow photosynthetically. Cells evolved O_2 at rates 40–60% those observed in cells with wild-type D1 protein, and showed rapid electron transfer to the Q_B-site for both odd and even flashes. However, the rate on the first flash was slower than that on the second, reversing the pattern of the binary oscillation in the fluorescence yield measured at ~200 μs after each of a series of flashes. Both His252Asn and His252Gln showed some rapid electron transfer from Q_A^- to Q_B following the first actinic flash after dark-adaptation, but with a reduced yield. Both were severely inhibited on the second flash. His252Lys was severely inhibited even after the first flash. Thermoluminescence studies after illumination with 1 saturating flash immediately before freezing showed glow-curves for all strains in which the peak was shifted to higher temperatures. From this we conclude than even in the strongly inhibited His252Lys strain, some electron transfer to Q_B occurred.

The pattern of dependence of electron transfer rate on flash number observed at pH 7.0 with His252Asp was similar to that seen in wild-type at pH above the pK at 8.0 for the Q_B^- state. This suggests that in His252Asp, a pK shift similar to that in wild-type might be occurring, but starting with a pK in the dark lower than that in wild-type, as might be expected for the more acidic aspartate side chain. The rapid electron transfer after the first flash observed with strains His252Gln and His252Asn shows that reduction of Q_B was not dependent on delivery of a proton to the site through this pathway. The strongly inhibited rate after the second flash can be readily interpreted as showing that transfer of the second electron has to wait for binding of the first proton (Wraight, 1979), dependent on a dissociable group at this site. The behavior of these mutant strains supports the suggestion of a role for His252 in proton delivery to the Q_B-site. We are currently investigating the pH dependence of rates and equilibrium constants for the electron transfer from Q_A^- to Q_B in these strains to further test this hypothesis.

5. Excision of Residues from the PEST Sequence of the **de***-Loop*

The span leading from the top of helix **D** to the **de** helix contains a sequence called the 'PEST-like' region (Greenberg et al., 1987), which has been suggested as a likely site for proteolysis in the turnover of D1 associated with photoprotection. Nixon at al. (1995) deleted a substantial span (residues 226-233) in this region, and showed that the resultant strain was able to grow photosynthetically, with light-saturated rates similar to wild type. Remarkably, electron transfer on the acceptor side was still rapid, despite excision of this substantial section of the **de**-loop, and the likely structural consequences. Not surprisingly, the properties of the site were modified, and measurements using thermoluminescence and fluorescence yield kinetic changes showed that Q_B^- was destabilized relative to Q_A^-. Measurements of D1 turnover showed an enhanced turnover in the deletion strain indicating that the PEST sequence was not required. Similar deletion studies have been reported by Mulo and co-workers (1997, 1998), in which excision of span 225-239 resulted in an autotrophic strain with a functional but modified Q_B-site, and with a similar susceptibility to photoinhibition to wild type. Excision of spans 225-249 or 240-249 gave heterotrophic strains with modified Q_B-pockets, severely inhibited electron transfer, and impaired recovery from photoinhibition. The authors concluded that no specific sequence in the **de**-loop was essential for D1 polypeptide degradation. The Ferreira et al. (2004) structure shows that the loop between 225 and 249 is well removed from the Q_B-site, consistent with the lack of effect on two-electron gate function shown by these results.

6. Mutagenesis to Explore the Bicarbonate Effect

Govindjee and colleagues have used specific mutagenesis in *Synechocystis* and *Chlamydomonas* to test the hypothesis that arginine residues in the neighborhood of the quinone binding sites might serve as ligands to bicarbonate. Mutation of D1-Arg269 to glycine in led to substantial changes in stability of the complex, 17-fold change in rate of electron transfer from Q_A^- to Q_B, loss of thermoluminescence peaks, but not to any change in formate/bicarbonate binding as judged from the $Q_A^-.Fe^{2+}$ EPR signal (Hutchison et al., 1996; Xiong et al., 1997). Mutation at Arg257 (Xiong et al., 1998b) to glutamate (Arg257Glu) or methionine (Arg257Met) were able to function with near normal kinetics of electron transfer between the Q_A and Q_B sites, but with a somewhat reduced equilibrium constant for the forward reaction. Interestingly, both mutations led to greatly reduced sensitivity to inhibition by incubation with formate, which displaced bicarbonate in native strains. Several of single and double mutants in the **de**-helix and the loop around Ser264 in *Synechocystis* PCC 6714 showed similar differential effects on formate sensitivity (Vernotte et al., 1995 or 1993). Since the bicarbonate effect is normally studied through the formate effect (Blubaugh and Govindjee, 1988; van Rensen et al, 1999; van Rensen, 2002), conclusions about the role of any of these residues in binding of bicarbonate must remain tentative.

E. Effects of Occupation of the Q_B-site on the E_m for Q_A and on the Equilibrium Constants in the Two-Electron Gate

Many reports have been published showing changes in E_m of the Q_A/Q_A^- couple on addition of inhibitors that bind to the Q_B-site, both in BRCs and PS II. Although most workers had assumed that any effects with DCMU were small, recent work has suggested that this might not be the case (Krieger-Liszkay and Rutherford, 1998). For example, the E_m for Q_A/Q_A^- is shifted from –70 to –30 mV by DCMU, and to –130 mV in the presence of bromoxynil. An interesting discussion of these effects in the light of the sensitivity to photo-oxidative damage has recently been published (Rutherford and Krieger-Liszkay, 2001, 2002; Fufezan et al., 2002). It should be noted that values for K_{app} calculated using the kinetic approach above depend on the assumption that the E_m value of the Q_A couple is the same whether the Q_B-site is occupied by DCMU or by the $Q_B/Q_B^{\cdot -}$ couple; the potential of Q_A in the absence of inhibitor as always measured with QH_2 in the site. A change in E_m for the Q_A/Q_A^- couple changes the probability for population of different intermediate states, and should therefore affect the back reaction rate measured. It is not clear how large an effect this would be compared to that arising from occupancy by Q_B, but the K_{app} values measured from the ratio of back reaction rates will likely have to be corrected. In addition, estimation of the E_m for the $Q_B/Q_B^{\cdot -}$ couple from the equilibrium constant depends directly on the value assumed for E_m Q_A/Q_A^-. In a recent study, Rappaport et al. (2002)

measured the back reaction rates from Q_A^- to P^+ in strains in which the free-energy gap between Q_A and the intermediate pheophytin acceptor (Pheo) of the photochemical reaction was varied. Their analysis has called into question the commonly assumed values for midpoint potentials of the Q_A/Q_A^-, Pheo/Pheo$^-$, and P^+/P couples. These recent developments will open this area to further revision, and perhaps some reinterpretation of earlier work.

Although Q_A acts as a single electron acceptor under physiological conditions, double reduction is possible under extreme reducing conditions (see van Mieghem et al, 1989, for a reinterpretation of the observations of Evans et al., 1985). Diner and Babcock (1996) present a critical discussion of the related literature.

F. Role of the Q_B-Site in Back-Reactions to the S-States

1. Back Reaction from Q_B^- to the S_2-State

The back reaction after a single flash from the dark-adapted state ($S_2Q_B^-$ back reaction) can be assayed by fluorescence measurements, as discussed at length in the context of the kinetic model above. The reaction has also been studied extensively through relaxation of the S_2-state, and through delayed fluorescence, thermoluminescence, and electroluminescence (Bowes and Crofts, 1979; van Gorkom, 1996; Vass and Govindjee, 1996; de Wijn et al., 2001). The overall reaction is close to stoichiometric in yield, but energy levels strongly affect the path, especially the fraction of centers decaying through pathways populating the excited state. Since the rate observed through fluorescence yield experiments and S_2-state deactivation are similar, and since the equilibrium constant calculated as above, and from thermoluminescence, are similar, a back reaction via Q_A^- and pheophytin is generally assumed, generating a small fraction of intermediate states with sufficient energy to populate the singlet level to give delayed fluorescence or thermoluminescence (Crofts et al, 1971; Bowes and Crofts, 1981b; Rutherford et al., 1982; Demeter et al, 1993; Johnson et al, 1994; Krieger et al, 1998).

2. Back Reaction from QH_2 to the S_3-State—A Possible Role for Cytochrome b_{559}

The relaxation of the S_3-state generated by two-flash excitation from the dark-adapted state, as measured by O_2 yield, shows kinetics similar to that of the S_2 relaxation (Diner, 1977). However, in this case, the source of electrons is not obvious. The acceptor side complex evolves to the initial state (Q_AQ_B or Q_A.vacant) within 4 ms after two flashes, leaving the two reducing equivalents as QH_2 in the pool (Robinson and Crofts, 1987). The E_m of the pool is ~100 mV, so the probability of re-population of the reduced acceptor complex would be low (from the values above, at neutral pH, K_{eq} for the reaction $Q_A.Q_B + QH_2 \leftrightarrows Q_A^-Q_B^- + Q + 2\,H^+$ is ~ 10^{-3}). Moreover, Diner (1977) found that the rate of the back reaction after two flashes ($Q_B^{2-}S_3 \rightarrow Q_B^-S_2$) was only weakly dependent on the degree of reduction of the quinone pool, suggesting that this is not the pathway. An alternative source of electrons would be from the endogenous reductants (carotenoids, ancillary Chls, Cyt b_{559}) that are known to donate to P^+_{680} when the Mn-complex is disrupted. Since the equilibrium constants between P_{680} and the relevant S-state transitions are relatively small, this reductant pool would also be available to reduce the S_2 and S_3 states. However, no accumulation of the oxidized forms of these reductants is observed when the S-state system is intact (Diner, 1998). If they are involved, a pathway for their reduction from an additional pool must therefore be postulated. The obvious source is the quinone pool, and indeed, a DCMU-sensitive pathway for reduction of Cyt b_{559} has been demonstrated (Buser et al., 1992), and a plastoquinol oxidase activity involving Cyt b_{559} has been suggested (Kruk and Strzalka, 2001; Bondarava et al., 2003). From the inhibitor sensitivity, this must involve the Q_B-site. The structures currently available allow calculation of possible rate constants in putative steps. These show that the heme of Cyt b_{559} is ~24 Å from the expected position of Q_B. With a driving force of 250 mV, and a value for λ of 0.75 V, a rate constant of ~0.53 s^{-1}, assuming 100% occupancy, can be calculated using the Moser et al. (1995) equations. This is in line with measured values for rates of deactivation, and a plausible occupancy. The most likely acceptor would be the ancillary Chl of D2, liganded by His117, since mutation of the ligand leads to loss of Chl photooxidation (Chl Z^+) (Ruffle et al., 2001). The edge-to-edge distance between heme b_{559} and this Chl is ~21.5 Å; with a driving force of ~400 mV, and any reasonable value for λ, this step would not be rate-limiting. In this simple scenario, electrons for reduction of both the S-states could follow the same pathway through Cyt b_{559}, since the Q_B^- would be a better substrate than QH_2 for reduction of Q_A.

An alternative and in some ways more attractive mechanism, using a similar reaction pathway, is for the Q_B-site to catalyze an 'oxidant-induced reduction' reaction:

$$QH_2 + \text{Cyt } b_{559} + Q_A \leftrightarrows Q + \text{Cyt } b^-_{559} + Q_A^- + 2H^+$$

The reaction would proceed via an intermediate $Q_AQ_B^-$ state, in which the semiquinone would be sufficiently reducing to force the second electron onto Q_A (the overall equilibrium constant would be ~10^3), thus providing parallel pathways for the two electrons, one of which would return via Cyt b_{559} and Chl Z, and the other via Q_A^- and the normal S_2 deactivation pathway.

$$S_3 + Chl_Z \rightarrow S_2 + Chl_Z^+$$

$$Chl_Z^+ + \text{Cyt } b^-_{559} \rightarrow Chl_Z + \text{Cyt } b_{559}$$

$$QH_2 + \text{Cyt } b_{559} + Q_A \leftrightarrows \text{Cyt } b^-_{559} + Q_AQ_B^- + 2H^+$$

$$Q_AQ_B^- \leftrightarrows Q_A^-Q_B \leftrightarrows Q_A^- + Q$$

$$S_2 + Q_A^- \rightarrow S_1 + Q_A$$

$$S_3 + QH_2 \rightarrow S_1 + Q + 2H^+$$

Discrimination between these two possibilities might not be easy, since in both cases, deactivation of the S_3-state would involve electron transfer from plastoquinol to S_3 via Cyt b_{559}. However, an involvement of both Cyt b_{559} and the ancillary D2 Chl, Chl_Z, could be readily tested by observation of the S_3 decay kinetics in mutant strains with the ligands to these two groups modified (Morais et al., 2001; Ruffle et al., 2001).

A role for interaction between the Q_B-site and Cyt b_{559} in the protein processing consequent on photodamage is suggested by an interesting study of a covalent bond formed between b_{559} and D1 through His252 (Lupinkova et al., 2002).

Deactivation of the higher S-states by the back reaction plays an obvious role in removal of potentially harmful oxidants. Less obvious is the fact that this also removes potentially harmful reductants, – Q_A^- has a reducing potential in the range to generate superoxide by reduction of O_2, and even the Q_B/Q_B^- couple reacts with O_2 at a low rate, as seen in the slowed kinetics for oxidation under anaerobic conditions when the back reaction is prevented by hydroxylamine (H. H. Robinson and A. R. Crofts, unpublished). Ohad and colleagues (Keren et al., 1997) have examined the inactivation of PS II under flash illumination at a repetition rate in the range of the lifetime of the Q_A^- and Q_B^- states back reacting with S_2 or S_3. Inactivation, or D1 degradation, showed a dependence on the interval between flashes, with half-maximal effects at ~50 s (compared to $t_{½}$ ~7 s for the back reaction from Q_A^-) in the presence of DCMU, and ~150 s (compared to the back reaction time from Q_B^- with $t_{½}$ ~ 35 s). The inactivation was much less under anaerobic conditions, showing a requirement for O_2. The authors interpreted the data as showing a mechanism in which the back reaction generates damaging oxygen radicals through involvement of the Chl triplet. However, it seems possible that a direct reduction of O_2 by the reduced acceptor quinones might provide an alternative mechanism. These topics are discussed in greater detail elsewhere in this volume.

IV. Conclusions

The structural information from spectroscopy, specific mutagenesis, kinetic studies and modeling has been remarkably successful in predicting specific structural features relating to the mechanism of the two-electron gate, now revealed by crystallographic studies. This success may be viewed as validating these approaches, but also provides some confidence in the kinetic models, and the conclusions drawn from them. With more detailed structures, the scope for future work in which the molecular architecture of the two-electron gate is explored through a combination of these approaches holds the promise of a detailed understanding of the reactions on the acceptor side of PS II.

Acknowledgments

V.P. acknowledges insightful discussions with Drs N. Ioannidis and Y. Sanakis. Research support for the lab of V.P. was provided through the EC programs ERBFMRXCT980214, and ERBFMRXCT980174. A.R.C. acknowledges earlier support from DOE and USDA that covered the research work discussed in the second part, the major contributions of Dr. Howie Robinson and Shinichi Taoka to development of the

kinetic models discussed, and more recent useful discussions with Dr. Vlad Shinkarev.

References

Aasa R, Andreasson L-E, Styring S and Vanngard T (1989) The nature of the Fe(III) EPR signal from the acceptor-side iron in Photosystem II. FEBS Lett 243: 156–160

Aiach A, Ohmann E, Bodner U and Johanningmeier U (1992) A herbicide resistant *Euglena* mutant carrying a Ser to Thr substitution of position 265 in the D1 protein of Photosystem II. Z Naturforsch 47c: 245–248.

Ajlani G, Kirilovsky D, Picaud M and Astier C (1989a) Molecular analysis of *psbA* mutations responsible for various herbicide resistance phenotypes in *Synechocystis* 6714. Plant Mol Biol 13: 469–480

Ajlani G, Meyer I, Vemotte C and Astier C (1989b) Mutation in phenol-type herbicide resistance maps within the *psbA* gene in *Synechocystis* 6714. FEBS Lett 246: 207– 210

Alfonso M, Pueyo JJ, Gaddour K, Etienne AL, Kirilovsky D and Picorel R (1996) Induced new mutation of D1 serine-268 in soybean photosynthetic cell cultures produced atrazine resistance, increased stability of $S_2Q_B^-$ and $S_3Q_B^-$ states, and increased sensitivity to light stress. Plant Physiol 112: 1499–1508

Allen JP, Feher G, Yeates TO, Komiya H and Rees DC (1988) Structure of the reaction center from *Rhodobacter sphaeroides* R-26: Protein-cofactor (quinones and Fe^{2+}) interactions. Proc Nat Acad Sci USA 85: 8487–8491

Anderson BF, Baker HM, Norris GE, Rice DW and Baker EN (1989) Structure of human lactoferrin: Crystallographic structure analysis and refinement at 2.8 Å resolution. J Mol Biol 209: 711–734

Astashkin AY, Kawamori A, Kodera Y, Kuroiwa S and Akabori K (1995) An electron spin echo envelope modulation study of the primary acceptor quinone in Zn-substituted plant Photosystem II. J Chem Phys 102: 5583–5588

Astashkin AV, Hara H, Kuroiwa S, Kawamori A and Akabori K (1998) A comparative electron spin echo envelope modulation study of the primary electron acceptor quinone in Zn-substituted and cyanide-treated preparations of Photosystem II. J Chem Phys 108: 10143–10151.

Astier C, Meyer I, Vernotte C and Etienne A-L (1986) Photosystem II electron transfer in highly herbicide resistant mutants of *Synechocystis* 6714. FEBS Lett 207: 234–238

Astier C, Perewoska I, Picaud M, Kirilovsky D and Vernotte C (1993) Structural analysis of the Q_B pocket of the D1 subunit of Photosystem II in *Synechocystis* PCC6714 and 6803. Z Naturforsch 43c: 199–204

Baroli I (1992) The two-electron gate of Photosystem II in wild type and herbicide-resistant mutants of *C. reinhardtii.* MSc Thesis, University of Illinois

Beijer C and Rutherford AW (1987) The iron-quinone acceptor complex in *Rhodospirillum rubrum* chromatophores studied by EPR. Biochim Biophys Acta 890: 169–178

Berthomieu C and Hienerwadel R (2001) Iron coordination in Photosystem II: Interaction between bicarbonate and the Q_B pocket studied by Fourier transform infrared spectroscopy. Biochemistry 40: 4044–4052

Bettini P, McNally S, Sevignac M, Darmency H, Gasquez J and Dron M (1987) Atrazine resistance in *Chenopodium album*: Low and high levels of resistance to the herbicide are related to the same chloroplast PSBA gene mutation. Plant Physiol 84: 1442–1446

Blubaugh D and Govindjee (1988) The molecular mechanism of the bicarbonate effect at the plastoquinone reductase site of photosynthesis. Photosynth Res 19: 85–128

Boinnard D, Cassoux P, Petrouleas V, Savariault JM and Tuchagues JP (1990) Iron(II) complexes of 2,2′-biimidazole and 2,2′-bibenzimidazole as models of the photosynthetic mononuclear non-heme ferrous sites. Synthesis, molecular and crystal structure, and Mossbauer and magnetic studies. Inorg Chem 29: 4114–4122

Bondarava N, De Pascalis L, Al-Babili S, Goussias C, Golecki JR, Beyer P, Bock R and Krieger-Liszkay A (2003) Evidence that Cyt b_{559} mediates the oxidation of reduced plastoquinone in the dark. J Biol Chem 278:13554–13560

Boso B, Debrunner P, Okamura MY and Feher G (1981) Mossbauer spectroscopy studies of photosynthetic reaction centers from *Rhodopseudomonas sphaeroides* R-26. Biochim Biophys Acta 638: 173–177

Bowes JM and Crofts AR (1980) Binary oscillations in the rate of reoxidation of the primary acceptor of Photosystem II. Biochim Biophys Acta 590: 373–384

Bowes JM and Crofts AR (1981a) Effect of DBMIB on the secondary electron acceptor B of Photosystem II. Arch Biochem Biophys 209: 682–686

Bowes JM and Crofts AR (1981b) The role of pH and membrane potential in the reactions of Photosystem II as measured by effects on delayed fluorescence. Biochim Biophys Acta 637: 464–472

Bowes JM, Crofts AR and Itoh S (1979a) A high potential acceptor for photosystern II. Biochim Biophys Acta 547: 327–335

Bowes JM, Crofts AR and Itoh S (1979b) Effects of pH on reactions on the donor side of Photosystem II. Biochim Biophys Acta 547: 336–346

Bowes JM, Crofts AR and Arntzen CJ (1980) Redox reactions on the reducing side of Photosystem II in chloroplasts with altered herbicide binding properties. Arch Biochem Biophys 200: 303–308

Bowyer J, Hilton M, Whitelegge J, Jewess P, Camilleri P, Crofts AR and Robinson HH (1990) Molecular modelling studies on the binding of phenylurea inhibitors to the D1 protein of Photosystem II. Z Naturforsch 45c: 379–387

Bowyer JR, Camilleri P and Vermaas WFJ (1991) Photosystem II and its interaction with herbicides. In: Baker NR and Percival MP (eds) Topics in Photosynthesis, Vol 10, Herbicides, pp 27–85. Elsevier Science Publishers BV, Amsterdam

Breton J, Boullais C, Mioskowski C, Sebban P, Baciou L and Nabedryk E (2002) Vibrational spectroscopy favors a unique Q_B binding site at the proximal position in wild-type reaction centers and in the Pro-l209 → Tyr mutant from *Rhodobacter sphaeroides*. Biochemistry 41: 12921–12927

Burda K, Kruk J, Borgstadt R, Stanek J, Strzalka K, Schmid GH and Kruse O (2003) Mossbauer studies of the non-heme iron and cytochrome b_{559} in a *Chlamydomonas reinhardtii* PS I^- mutant and their interactions with α-tocopherol quinone. FEBS Lett 535: 159–165

Buser CA, Diner BA and Brudvig GW (1992) Photooxidation of cytochrome *b*-559 in oxygen-evolving Photosystem II. Biochemistry 31: 11449–11459

Cleland RE and Grace SC (1999) Voltammetric detection of superoxide production by Photosystem II. FEBS Lett 457: 348–352

Crofts AR and Wraight CA (1983) The electrochemical domain of photosynthesis. Biochim Biophys Acta 726: 149–185

Crofts AR, Wraight CA and Fleischman DE (1971) Energy conservation in the photochemical reactions of photosynthesis and its relation to delayed fluorescence. FEBS Lett 15: 89–100

Crofts AR, Robinson HH and Snozzi M (1984) Reactions of quinols at catalytic sites; a diffusional role in H-transfer. In: Sybesma C (ed) Advances in Photosynthesis Research, Vol I, pp 461–468. Martinus Nijhoff/Dr W Junk, The Hague

Crofts AR, Robinson HH, Andrews K, Van Doren S and Berry E (1987) Catalytic sites for reduction and oxidation of quinones. In: Papa S, Chance B and Ernster L (eds) Cytochrome Systems: Molecular Biology and Bioenergetics, pp 617–624. Plenum Publ Corp, New York

Crofts AR, Baroli I, Kramer D and Taoka S (1993) Kinetics of electron transfer between Q_a and Q_b in wild-type and herbicide-resistant mutants of *C. reinhardtii*. Z Naturforsch 48c: 259–266

de Wijn R and van Gorkom HJ (2001) Kinetics of electron transfer from Q_A to Q_B in Photosystem II. Biochemistry 40: 11912–11922

de Wijn R, Schrama T and van Gorkom HJ (2001) Secondary stabilization reactions and proton-coupled electron transport in Photosystem II investigated by electroluminescence and fluorescence spectroscopy. Biochemistry 40: 5821–5834

Debrunner, PG (1996) Mossbauer spectroscopy. In: Amesz J and Hoff J (eds) Biophysical Techniques in Photosynthesis, pp 355–373. Kluwer Academic Publishers, Dordrecht

Debrunner PG, Schulz CE, Feher G and Okamura MY (1975) Mossbauer study of reaction centers from *R. sphaeroides*. Biophys J 15: 226a.

Deisenhofer J and Michel H (1989) The photosynthetic reaction center from the purple bacterium *Rhodopseudomonas viridis.* Science 245: 1463–1473

Deisenhofer J, Epp O, Miki K, Huber R and Michel H (1985) Structure of the protein subunits in the photosynthetic reaction centre of *Rhodopseudomonas viridis* at 3 Å resolution. Nature 318: 618–624

Deisenhofer J, Epp O, Sinning I and Michel H (1995) Crystallographic refinement at 2.3-angstrom resolution and refined model of the photosynthetic reaction centre from *Rhodopseudomonas viridis*. J Mol Biol 246: 429–457

Deligiannakis Y, Tsekos N, Petrouleas V and Diner BA (1992) Orientation dependence of the Fe^{2+}-NO and Fe^{3+} EPR signal associated with the non-heme iron of Photosystem II. Biochim Biophys Acta 1140: 163–168

Deligiannakis Y, Petrouleas V and Diner BA (1994) Binding of carboxylate anions at the non-heme Fe(II) of PS II. I Effects on the $Q_A^-Fe^{2+}$ and Q_AFe^{3+} EPR spectra and the redox properties of the iron. Biochim Biophys Acta 1188: 260–270

Deligiannakis Y, Boussac A and Rutherford AW (1995) ESEEM study of the plastoquinone anion radical ($Q_A^{\bullet -}$) in ^{14}N- and ^{15}N-labeled Photosystem II treated with CN^-. Biochemistry 34: 16030–16038

Deligiannakis Y, Jegerschold C and Rutherford AW (1997) EPR and ESEEM study of the plastoquinone anion radical Q_A^- in Photosystem II treated at high pH. Chem Phys Lett 270: 564–572

Deligiannakis Y, Ioannidis N and Petrouleas V (1998) lD- and 2D-ESEEM study of the [Fe-NO](S=3/2) complex of PS II. In Garab G (ed): Photosynthesis: Mechanisms and Effects, Vol II, pp 1117–1120. Kluwer Academic Publishers, Dordrecht

Deligiannakis Y, Hanley, J and Rutherford AW (1999) lD- and 2D-ESEEM study of the semiquinone radical Q_A^- of Photosystem II. J Am Chem Soc 121: 7653–7664

Demeter S, Goussias Ch, Bemat G, Kovacs L and Petrouleas V (1993), Participation of the g = 1.9 and g = 1.82 EPR forms of the semiquinone-iron complex, $Q_A^-Fe^{2+}$ of Photosystem II in the generation of the Q and C thermoluminescence bands, respectively. FEBS Lett 336: 352–356

Diner BA (1977) Dependence of the deactivation reactions of Photosystem II on the redox state of the plastoquinone pool A, varied under anaerobic conditions. Equilibria on the acceptor side of Photosystem II. Biochim Biophys Acta 460: 247–258

Diner BA (1998) Application of spectroscopic techniques to the study of Photosystem II mutations engineered in *Synechocystis* and *Chlamydomonas*. Method Enzymol 297: 337–360

Diner BA and Babcock GT (1996) Structure, dynamics, and energy conversion efficiency in Photosystem II. In: Ort DR and Yocum CF (eds) Oxygenic Photosynthesis: The Light Reactions, pp 213–247. Kluwer Academic Publishers, Dordrecht

Diner BA and Petrouleas V (1987a) Light-induced oxidation of the acceptor-side Fe(lI) of Photosystem II by exogenous quinones acting through the Q_B binding site. II. Blockage by inhibitors and their effects on the Fe(III) EPR spectra. Biochim Biophys Acta 893: 138–148

Diner BA and Petrouleas V (1987b) Q_{400}, the non-heme iron of the Photosystem II iron-quinone complex. A spectroscopic probe of quinone and inhibitor binding to the reaction center. Biochim Biophys Acta 895: 107–125

Diner BA and Petrouleas V (1990) Formation by NO of nitrosyl adducts of redox components of the Photosystem II reaction center. II. Evidence that HCO_3^-/CO_2 binds to the acceptor-side non-heme iron. Biochim Biophys Acta 1015: 141–149

Diner BA, Petrouleas V and Wendoloski JJ (1991) The iron-quinone electron-acceptor complex of Photosystem II. Physiol Plant 81: 423–436

Draber W, Tietjen K, Kluth JF and Trebst A (1991) Herbicides in photosynthesis research. Angew Chem Int Ed Engl 30: 1621–1633

Draber W, Hilp U, Likusa H, Schindler M. and Trebst A (1993) Inhibition of photosynthesis by 4-nitro-6-alkyl-phenols: Structure-activity studies in wild-type and five mutants of *Chlamydomonas reinhardtii* thylakoids. Z Naturforsch 43c: 213–223

Dutton PL, Prince RC and Tiede DM (1978) The reaction center of photosynthetic bacteria. Photochem Photobiol 28: 939–949

Eaton-Rye JJ and Govindjee (1988) Electron transfer through the quinone acceptor complex of photosystern II after one or two actinic flashes in bicarbonate-depleted spinach thylakoid membranes. Biochim Biophys Acta 935: 248–257

Erickson JM, Rahire M, Bennoun P, Delepelaire P, Diner B and Rochaix JD (1984) Herbicide resistance in *Chlamydomonas reinhardtii* results from a mutation in the chloroplast gene for the 32 kDa protein of PS II. Proc Natl Acad Sci USA 81: 3617–3621

Erickson JM, Pfister K, Rahire M, Togasaki R, Mets L and Rochaix J-D (1989) Molecular and biophysical analysis of herbicide-resistant mutants of *Chlamydomonas reinhardtii:* Structure-

function relationship of the photosystern II Dl polypeptide. Plant Cell l: 361–371.

Etienne A-L, Ducruet J-M, Ajlani G and Vernotte C (1990) Comparative studies on electron transfer in Photosystem II of herbicide-resistant mutants from different organisms. Biochim Biophys Acta 1015: 435–440

Evans MCW, Atkinson YE and Ford RC (1985) Redox characterization of the photosystern II electron acceptors. Evidence for two electron carriers between pheophytin and Q. Biochim Biophys Acta 806: 247–254

Feher G and Okamura MY (1999) The primary and secondary acceptors in bacterial photosynthesis. Appl Magn Reson 16: 63–100

Ferreira KN, Iverson TM, Maghlaoui K, Barber J and Iwata S (2004) Architecture of the Photosynthetic Oxygen-Evolving Center. Science 303: 1831-1838

Forster B, Heifetz PB, Lardans A, Boynton JE, Gillham NW (1997) Herbicide resistance and growth of D1 Ala(251) mutants in *Chlamydomonas*. Z Naturforsch 52c: 9–10

Fowler CF (1977) Proton translocation in chloroplasts and its relationship to electron transport between the photosystems. Biochim Biophys Acta 459: 351–363

Fritzsch G, Kampmann L, Kapaun G and Michel H (1998) Water clusters in the reaction centre of *Rhodobacter sphaeroides*. Photosynth. Res. 55: 1–6.

Fufezan C, Rutherford AW and Krieger-Liszkay A (2002) Singlet oxygen production in herbicide-treated Photosystem II. FEBS Lett. 532: 407–410

Galloway R and Mets LJ (1984) Atrazine, bromacil and diuron resistance in *Chlamydomonas*. A single non-mendelian genetic locus controls the structure of the thylakoid binding site. Plant Physiol 74: 469–474

Garbers A, Reifarth F, Kurreck J, Renger G and Parak F (1998) Correlation between protein flexibility and electron transfer from Q_A^- to Q_B in PS II membrane fragments from spinach. Biochemistry 37: 11399–11404

Garge P, Chikate R, Padhye S, Savariault JM, de Loth P and Tuchagues J-P (1990) Iron(II) complexes of ortho-functionalized para-naphtoquinones. 2. Crystal and molecular structure of bis(aquo)bis(lawsone)iron(II) and intermolecular magnetic exchange interactions in bis(3-aminolawsone)iron(II). Inorg Chem 29: 3315–3320

Golden SS and Haselkorn R (1985) Mutation to herbicide resistance maps within the *psb*A gene of *Anacystis nidulans* R2. Science 229: 1104–1107

Goussias CH, Deligiannakis Y, Sanakis Y, Ioannidis N, and Petrouleas V (2002) Probing subtle coordination changes in the iron- quinone complex of Photosystem II during electron transfer, by the use of NO. Biochemistry 41: 15212–152233

Govindjee (1990) Photosystem II heterogeneity: The acceptor side. Photosynth Res 25: 151-160

Govindjee, Eggenberg P, Pfister K and Stasser RJ (1992) Chlorophyll *a* fluorescence decay in herbicide-resistant D1 mutants of *Chlamydomonas reinhardtii* and the formate effect. Biochim Biophys Acta 1101: 353–358

Greenberg BM, Gaba V, Mattoo AK and Edelman M (1987) Identification of a primary in vivo degradation product of the rapidly-turning-over 32-kD protein of Photosystem II. EMBO J 6: 2865–2869

Hallahan BJ, Ruffle SV, Bowden SJ and Nugent JHA (1991) Identification and characterisation of EPR signals involving Q_B semiquinone in plant Photosystem II. Biochim Biophys Acta 1059: 181–188

Haumann M and Junge W (1994) The rates of proton uptake and electron transfer at the reducing side of Photosystem II in thylakoids. FEBS Lett 347: 45–50

Heathcote P and Rutherford AW (1987) An E.P.R. signal arising from Q_B^-Fe in *Chromatium vinosum* strain D. In: Biggins J (ed) Progress in Photosynthesis Research, Vol I, pp 201–204. Martinus Nijhoff Publisher, Dordrecht

Hegg EL and Que L Jr (1997) The 2-His-1-carboxylate facial triad. An emerging structural motif in mononuclear non-heme iron(II) enzymes. Eur J Biochem 250: 625–629

Hienerwadel R and Berthomieu C (1995) Bicarbonate binding to the non-heme iron of Photosystem II investigated by Fourier transform infrared difference spectroscopy and ^{13}C-labeled bicarbonate. Biochemistry 34: 16288–16297

Hirschberg J and McIntosh L (1983) Molecular basis of herbicide resistance in *Amaranthus hybridus*. Science 222:1346–1349

Hope AB and Matthews DB (1983) Further studies on proton translocations in chloroplasts after single-turnover flashes: 1. Proton uptake. Aust J Plant Physiol 10: 363–372

Hope A and Morland A (1979) Proton Translocation in isolated spinach chloroplasts after single-turnover actinic flashes. Aust J Plant Physiol 6: 289–304

Hubbard JAM, Corrie AR, Nugent JHA and Evans MCW (1989) Properties of the Photosystem II electron acceptor complex of *Phormidium laminosum*. Biochim. Biophys. Acta 977: 91–96

Huppatz JL (1996) Quantifying the inhibitor-target site interactions of Photosystem II herbicides. Weed Science 44: 743-748

Huppatz JL and Phillips JN (1984) Cyanoacrylate inhibitors of the Hill reaction. III. Stereochemical and electronic aspects of inhibitor binding. Z Naturforsch 39c: 617–622

Hutchison RS, Xiong J, Sayre RT and Govindjee (1996) Construction and characterization of a Photosystem II D1 mutant (arginine-269-glycine) of *Chlamydomonas reinhardtii*. Biochim Biophys Acta 1277: 83–92

Ikegami and Katoh S (1973) Studies on chlorophyll fluorescence in chloroplasts II. Effect of ferricyanide on the induction of fluorescence in the presence of 3-(3,4-dichlorophenyl)-1,1-dimethylurea. Plant Cell Physiol 14: 829–836

Itoh S, Tang XS and Satoh K (1986) Interaction of the high spin Fe atom in the photosystern II reaction center with the quinones Q_A and Q_B in purified oxygen-evolving PS II reaction center complex and in PS II particles. FEBS Lett 205: 275–281

Johanningmeier U, Sopp G, Brauner M, Altenfeld U, Orawski G, Oettmeier W (2000) Herbicide resistance and supersensitivity in Ala(250) or Ala(251) mutants of the D1 protein in *Chlamydomonas reinhardtii*. Pesticide Biochem Physiol 66: 9–19

Johnson GN, Boussac A and Rutherford AW (1994) The origin of 40–50 °C thermoluminescence bands in Photosystem II. Biochim Biophys Acta 1184: 85–92

Joliot P (1974) Effect of low temperature (–30 to –60 °C) on the reoxidation of the Photosystem II primary electron transfer in the presence and absence of 3(3,4-dichlorophenyl)-1,1-dimethylurea. Biochim. Biophys. Acta 357: 439–448

Joliot P, Lavergne J and Beal D (1992) Plastoquinone compartmentation in chloroplasts: I. Evidence for domains with different rates of photo-reduction. Biochim Biophys Acta 1101: 1–12

Kaminskaya, OP, Drachev LA, Konstantinov AA, Semenov AY and

Skulachev VP (1986) Electrogenic reduction of the secondary quinone acceptor in chromatophores of *Rhodospirillum rubrum:* Rapid kinetic measurements. FEBS Lett 202: 224–228

Kamiya N and Shen JR (2003) Crystal structure of oxygen-evolving Photosystem II from T*hermosynechococcus vulcanus* at 3.7-Å resolution. Proc Natl Acad Sci USA 100: 98–103

Kashino Y, Yamashita M, Okamoto Y, Koike H and Satoh K (1996) Mechanisms of electron flow through the Q_B site in Photosystem II. 3. Effects of the presence of membrane structure on the redox reactions at the Q_B site. Plant Cell Physiol 37: 976–982

Keren N, Berg A, Vankan PJM, Levanon H and Ohad I (1997) Mechanism of Photosystem II photoinactivation and D1 protein degradation at low light — the role of back electron flow. Proc Natl Acad Sci USA 94: 1579–1584

Kless H and Vermaas WFJ (1995) Many combinations of amino acid sequences in a conserved region of the D1 protein satisfy Photosystem II function. J Mol Biol 246: 120–131

Kless H Oren-Shamir M, Ohad I, Edelman M and Vermaas WFJ (1993) Protein modifications in the D2 protein of Photosystem II affect properties of the Q_B/herbicide binding environment. Z Naturforsch 43c: 170–184

Klimov VV, Dolan E, Shaw ER and Ke B (1980) Interaction between the intermediary electron acceptor (pheophytin) and a possible plastoquinone-iron complex in Photosystem II reaction centers. Proc Natl Acad Sci USA 77: 7227–7231

Koulougliotis D, Kostopoulos T, Petrouleas V and Diner BA (1993) Evidence for CN-binding at the PS II non-heme Fe^{2+}. Effects on the EPR signal for $Q_A^-Fe^{2+}$ and on Q_A/Q_B electron transfer. Biochim Biophys Acta 1141: 275–282

Krieger A, Rutherford AW and Jegerschold C (1998) Thermoluminescence measurements on chloride-depleted and calcium-depleted Photosystem II. Biochim Biophys Acta 1364: 46–54

Krieger-Liszkay A and Rutherford AW (1998) Influence of herbicide binding on the redox potential of the quinone acceptor in Photosystem II: Relevance to photodamage and phytotoxicity. Biochemistry 37: 17339-17344

Kruk J and Strzalka K (2002) Redox changes of cytochrome b_{559} in the presence of plastoquinones. J Biol Chem 276: 86-91

Kuglstatter A, Ermler U, Michel H, Baciou L and Fritzsch G (2001) X-ray structure analyses of photosynthetic reaction center variants from *Rhodobacter sphaeroides*: Structural changes induced by point mutations at position L209 modulate electron and proton transfer. Biochemistry 40: 4253–4260

Kurreck J, Garbers A, Reifarth F, Andreasson L-E, Parak F, Renger G (1996) Isolation and properties of PS II membrane fragments depleted of the non heme iron center. FEBS Letters 381: 53–57

Lancaster CRD and Michel H (1997) The coupling of light-induced electron transfer and proton uptake as derived from crystal structures of reaction centres from *Rhodopseudomonas viridis* modified at the binding site of the secondary quinone, Q_B. Structure 5: 1339–1359

Lancaster CRD and Michel H (1999) Refined structures of reaction centres from *Rhodopseudomonas viridi*s in complexes with the herbicide atrazine and two chiral atrazine derivatives also lead to a new model of the bound carotenoid. J Mol Biol 286: 883–898

Lardans A, Gillham NW, Boynton JE (1997) Site-directed mutations at residue 251 of the Photosystem II D1 protein of *Chlamydomonas* that result in a nonphotosynthetic phenotype and impair D1 synthesis and accumulation. J Biol Chem 272: 210–216

Lavergne J (1982a) Interaction of exogenous benzoquinone with Photosystem II in chloroplasts: The semiquinone form acts as a dichlorophenyldimethylurea-insensitive secondary acceptor. Biochim Biophys Acta 679, 12–18

Lavergne J (1982b) Mode of action of 3-(3,4-dichlorophenyl)-1,1-dimethylurea: Evidence that the inhibitor competes with plastoquinone for binding to a common site on the acceptor side of Photosystem II. Biochim Biophys Acta 682: 345–353

Lavergne J (1982c) Two types of primary acceptors in chloroplast Photosystem II: I. Different recombination properties. Photobiochem Photobiophys 3: 257–271

Lavergne J, Bouchaud JP and Joliot, P. (1992) Plastoquinone compartmentation in chloroplasts: II. Theoretical aspects. Biochim Biophys Acta 1101: 13–22

Lipscomb JD and Orville AM (1992) Mechanistic aspects of dihydroxybenzoate dioxygenases. In: Sigel H and Sigel A (eds) Metal Ions in Biological Systems, Vol 28, pp 243–298. Marcel Dekker Inc, New York

Lupinkova L, Metz JG, Diner BA, Vass I and Komenda J (2002) Histidine residue 252 of the Photosystem II D1 polypeptide is involved in a light-induced cross-linking of the polypeptide with the alpha subunit of cytochrome *b*-559: Study of a site-directed mutant of *Synechocystis* PCC 6803. Biochim Biophys Acta 1554: 192–201

Macmillan F, Gleiter H, Renger G, Lubitz W (1990) EPR/ ENDOR studies of plastoquinone anion radical in Photosystem II (Q_A^-) and in organic solvents. In: Baltscheffsky M (ed) Current Research in Photosynthesis, Vol I, pp 531–534. Kluwer Academic Publishers, Dordrecht

MacMillan F, Kurreck I, Adir N, Lendzian F, Kass H, Reifarth F, Renger G and Lubitz W (1995a) EPR, ENDOR and ESEEM investigation of the electron acceptor radical anion $Q_A^{-\bullet}$ in photo system II (PS II) reaction centres. In Mathis P (ed) Photosynthesis: From Light to Biosphere, Vol I, pp 659–662. Kluwer Academic Publishers, Dordrecht

MacMillan F, Lendzian F, Renger G and Lubitz W (1995b) EPR and ENDOR investigation of the primary electron acceptor radical anion $Q_A^{\bullet -}$ in iron-depleted Photosystem II membrane fragments. Biochemistry 34: 8144–8156

Lorente M.A., Dahan F., Sanakis Y., Petrouleas V., Bousseksou A. and Tuchagues J. P. (1995) New ferrous complexes based on the 2,2′-biimidazole ligand: Structural, Mossbauer and Magnetic properties. Inorg. Chem. 34: 5346–5357

Michel H and Deisenhofer J (1988) Relevance of the photosynthetic reaction center from purple bacteria to the structure of Photosystem II. Biochemistry 27: 1–7

Michel H, Epp 0 and Deisenhofer J (1986) Pigment-protein interactions in the photosynthetic reaction centre from *Rhodopseudomonas viridis.* EMBO J 5: 2445–2451

Morais F, Kuhn K, Stewart DH, Barber J, Brudvig GW and Nixon PJ (2001) Photosynthetic water oxidation in cytochrome b_{559} mutants containing a disrupted heme-binding pocket. J Biol Chem 276: 31986–31993

Moreland DE (1993) Research on biochemistry of herbicides: An historical overview. Z. Naturforsch. 48c: 121–132

Moser CC, Page CC, Farid R and Dutton PL (1995) Biological electron transfer. J Bioenerg Biomemb 27: 263–274

Mulo P, Tyystjarvi T, Tyystjarvi E, Govindjee, Maenpaa P and Aro EM (1997) Mutagenesis of the d-e loop of Photosystem II

reaction centre protein D1 — function and assembly of Photosystem II. Plant Mol Biol 33: 1059–1071

Mulo P, Laakso S, Maenpaa P and Aro EM (1998) Stepwise photoinhibition of Photosystem II – studies with *Synechocystis* species PCC 6803 mutants with a modified de loop of the reaction center polypeptide D1. Plant Physiol 117: 483–490

Nabedryk E, Breton J, Sebban P and Baciou L (2003) Quinone (Q_B) binding site and protein structural changes in photosynthetic reaction center mutants at Pro-L209 revealed by vibrational spectroscopy. Biochemistry 42: 5819–5827

Nixon PJ, Komenda J, Barber J, Deak Z, Vass I and Diner BA (1995) Deletion of the PEST-like region of Photosystem II modifies the Q_B-binding pocket but does not prevent rapid turnover of D1. J Biol Chem 270: 14919–4927

Noguchi T, Kurreck J, Inoue Y and Renger G (1999a). Comparative FTIR analysis of the microenvironment of $Q_A^{-\bullet}$ in cyanide-treated, high pH-treated and iron-depleted Photosystem II membrane fragments. Biochemistry 38: 4846–4852

Noguchi T, Inoue Y, and Tang X-S (1999b). Hydrogen bonding interaction between the primary quinone acceptor Q_A and a histidine side chain in Photosystem II as revealed by Fourier transform infrared spectroscopy. Biochemistry 38: 399–403

Nugent JHA. (2001) Photoreducible high spin iron electron paramagnetic resonance signals in dark-adapted Photosystem II: Are they oxidised non-haem iron formed from interaction of oxygen with PS II electron acceptors? Biochim Biophys Acta 1504: 288–298

Nugent IHA, Diner BA and Evans MCW (1981) Direct detection of the electron acceptor of Photosystem 11. FEBS Lett 124: 241–244

Nugent JHA, Corrie AR, Demetriou C, Evans MCW and Lockett CJ (1988) Bicarbonate binding and the properties of Photosystem II electron acceptors. FEBS Lett 235: 71–75

Nugent JHA, Doetschman DC and Maclachlan DJ (1992) Characterization of the multiple EPR line shapes of iron-semiquinones in photosystem 2. Biochemistry 31: 2935–2941

Oettmeier W (1992) Herbicides of Photosystem II. In Barber J (ed) Topics in Photosynthesis Vol. 11: The Photosystems: Structure, Function and Molecular Biology, pp 349–408. Elsevier Science Publishers BV, Amsterdam

Oettmeier W (1999) Herbicide resistance and supersensitivity in Photosystem II. Cell Mol Life Sci 55: 1255–1277

Oettmeier W, Masson K, Kloos R and Reil E (1993) On the orientation of Photosystem II inhibitors in the Q_B-binding niche: Acridones, xanthones and quinones. Z Naturforsch 43c: 146–151

Okamura MY, Paddock ML, Graige MS and Feher G (2000) Proton and electron transfer in bacterial reaction centers. Biochim Biophys Acta 1458, 148–163

Orville AM and Lipscomb JD (1997) Cyanide and nitric oxide binding to reduced protocatechuate 3,4-dioxygenase: Insight into the basis for order-dependent ligand binding by intradiol catecholic dioxygenases. Biochemistry 36: 14044–14055

Peloquin JM, Tang X-S, Diner BA and Britt RD (1999) An electron spin-echo envelope modulation (ESEEM) study of the Q_A binding pocket of PS II reaction centers from spinach and *Synechocystis*. Biochemistry 38: 2057–2067

Petrouleas V and Diner BA (1982) Investigation of the iron components in Photosystem II by Mossbauer spectroscopy. FEBS Lett 147: 11–114

Petrouleas V and Diner BA (1986) Identification of Q_{400}, a high-potential electron acceptor of Photosystem II, with the iron of the quinone-iron acceptor complex. Biochim Biophys Acta 849: 264–275

Petrouleas V and Diner BA (1987) Light-induced oxidation of the acceptor-side Fe(II) of Photosystem II by exogenous quinones acting through the Q_B binding site. I. Quinones, kinetics and pH-dependence. Biochim Biophys Acta 893: 126–137

Petrouleas V and Diner BA (1990) Formation by NO of nitrosyl adducts of redox components of the Photosystem II reaction center. I. NO binds to the acceptor-side non-heme iron. Biochim Biophys Acta 1015: 131–140

Petrouleas V, Sanakis Y, Deligiannakis Y, Diner BA (1992) The non-heme Fe(II) of PS II: (1) Binding of new carboxylate anions, (2) Study of two Mossbauer components. In: Murata N (ed) Research in Photosynthesis, Vol II, 119–122. Kluwer Academic Publishers, Dordrecht

Petrouleas V, Deligiannakis Y, and Diner BA (1994) Binding of carboxylate anions at the non-heme Fe(II) of PS II. II. Competition with bicarbonate and effects on the Q_A/Q_B electron transfer rate. Biochim. Biophys. Acta 1188: 271–277

Picorel R, Williamson DL, Yruela I and Seibert M (1994) The state of iron in the oxygen-evolving core complex of the cyanobacterium *Phormidium laminosum:* Mossbauer spectroscopy. Biochim Biophys Acta 1184: 171–177

Polle A and Junge W (1986) The slow rise of the flash-light-induced alkalization by Photosystem II of the suspending medium of thylakoids is reversibly related to thylakoid stacking. Biochim Biophys Acta 848: 257—264

Pospısil P Arato A Krieger-Liszkay A and Rutherford AW (2004) Hydroxyl Radical Generation by Photosystem II Biochemistry ASAP.

Que L Jr (2000) One motif — many different reactions. Nature Struct Biol 7: 182–184

Que L Jr and Raymond YNH (1996) Dioxygen activation by enzymes with mononuclear non-heme iron active sites. Chem. Rev: 96, 2607–2624

Rakotonandrasana A, Boinnard D, Savariault JM, Tuchagues JP, Petrouleas V, Cartier C and Verdaguer M (1991) Iron(II) complexes with polydentate Schiff base ligands as models of the photosynthetic mononuclear non-heme ferrous sites. Synthesis, characterization, molecular crystal structure, EXAFS and XANES studies, Mossbauer spectroscopy and magnetic properties. Inorg Chim Acta 180: 19–31

Rappaport F, Guergova-Kuras M, Nixon PJ, Diner BA and Lavergne J (2002) Kinetics and pathways of charge recombination in Photosystem II. Biochemistry 41: 8518–8527

Reifarth F and Renger G (1998) Indirect evidence for structural changes coupled with $Q_B^{\bullet-}$ formation in Photosystem II. FEBS Lett 428: 123–126

Rigby SEJ, Heathcote P, Evans MCW and Nugent JHA (1995) ENDOR and special TRIPLE resonance spectroscopy of $Q_A^{\bullet-}$ of photosystem 2. Biochemistry 34: 12075-12081

Robinson HH and Crofts AR (1983) Kinetics of the oxidation-reduction reactions of the Photosystem II quinone acceptor complex, and the pathway for deactivation. FEBS Lett 153: 221–226

Robinson HH and Crofts AR (1984) Kinetics of proton uptake and the oxidation-reduction reactions of the quinone acceptor complex of Photosystem II from pea chloroplasts. In: Sybesma C (ed) Advances in Photosynthesis Research, Vol 1, pp 477–480. Martinus Nijhoff/ Dr W Junk Publishers, The Hague

Robinson, HH and Crofts AR (1987) Kinetics of the changes in oxidation-reduction states of the acceptors and donors of Photosystem II in pea thylakoids measured by flash fluorescence. In Biggins J (ed) Progress in Photosynthesis Research, Vol 2, pp 429–432. Martinus Nijhoff / Dr W Junk Publishers, The Hague

Robinson HH, Eaton-Rye JJ, van Rensen JJS and Govindjee (1984) The effects of bicarbonate depletion and formate incubation on the kinetics of oxidation-reduction reactions of the Photosystem II quinone acceptor complex. Z Naturforsch 39c: 382–385

Robinson HH, Golden S, Brusslan J and Haselkorn R (1987) Functioning of Photosystem II in mutant strains of the cyanobacterium *Anacystis nidulans* R2. In: Biggins J (ed) Progress in Photosynthesis Research, Vol IV, pp 825–828. Matinus Nijhoff Publishers, Dordrecht

Ruffle SV, Donnelly D, Blundell TL and Nugent JHA (1992) A three-dimensional model of the Photosystem II reaction centre of *Pisum sativum*. Photosynth Res 34: 287–300

Ruffle SV, Wang J, Johnston HG, Gustafson TL, Hutchison RS, Minagawa J, Crofts AR and Sayre RT (2001). Photosystem II peripheral accessory chlorophyll mutants in *Chlamydomonas reinhardti*i. Biochemical characterization and sensitivity to photo-inhibition. Plant Physiol 127: 633–644

Rutherford AW (1985) Orientation of EPR signals arising from components in Photosystem II membranes. Biochim Biophys Acta 807: 189–201

Rutherford AW (1987) How close is the analogy between the reaction centre of PS II and that of purple bacteria? 2. The electron acceptor side. In: Biggins J (ed) Progress in Photosynthesis Research, Vol 1, pp 277–283. Martinus Nijhoff Publishers, Dordrecht

Rutherford AW and Krieger-Liszkay A (2001) Herbicide-induced oxidative stress in Photosystem II. Trends Biol Sci 26: 648–653

Rutherford AW and Krieger-Liszkay A (2002) Singlet oxygen production in herbicide-treated Photosystem II. FEBS Lett 532: 407–-410

Rutherford AW and Zimmermann J-L (1984) A new EPR signal attributed to the primary plastoquinone acceptor in Photosystem II. Biochim Biophys Acta 767: 168–175

Rutherford AW, Crofts AR and Inoue Y (1982) Thermoluminescence as a probe of Photosystem II photochemistry; the origin of the flash induced glow peaks. Biochim Biophys Acta 682: 457–465

Sanakis Y and Petrouleas V (1995). Cyanide binding at the non heme iron of PS II and effects on certain EPR signals. In Mathis P (ed) Photosynthesis: From Light to Biosphere, Vol I, pp 823–826. Kluwer Academic Publishers, Dordrecht

Sanakis Y, Petrouleas V, and Diner BA (1994) Cyanide binding at the non-heme Fe^{2+} of the iron-quinone complex of Photosystem II: At high concentrations cyanide converts the Fe^{2+} from high ($S = 2$) to low ($S = 0$) spin. Biochemistry 33: 9922–9928

Sanakis Y, Petasis D, Petrouleas V and Hendrich M (1999) Simultaneous binding of fluoride and NO to the nonheme iron of Photosystem II: Quantitative EPR evidence for a weak exchange interaction between the semiquinone Q_A^- and the iron-nitrosyl complex. J Am Chem Soc, 121: 9155–9164

Saphon S and Crofts AR (1977) The H^+/e ratio in chloroplasts is 2. Possible errors in its determination. Z Naturforsch 32c: 810–816

Semin BK, Loviagina ER, Aleksandrov AY, Kaurov YN and Novakova AA (1990) Effect of formate on Mossbauer parameters of the non-heme iron of PS II particles of cyanobacteria. FEBS Lett 270: 184–186.

Shinkarev V and Wraight CA (1993) Electron and proton transfer in the acceptor quinone complex of reaction centers of photosynthetic bacteria. In Deisenhofer J (ed) The Photosynthetic Reaction Center, Vol 1, pp 193–255. Academic Press, New York

Snel JFH and van Rensen JJS. (1984) Reevaluation of the role of bicarbonate and formate in the regulation of photosynthetic electron flow in broken chloroplasts. Plant Physiol 75: 146–150

Spoyalov AP, Hulsebosch RJ, Shochat S, Gast P, Hoff AJ (1996) Evidence that Ala M260 is hydrogen-bonded to the reduced primary acceptor quinone $Q_A^{\bullet -}$ in reaction centers of *Rb. sphaeroides*. Chemical Physics Letters 263: 715–720

Stemler A and Murphy J (1983) Determination of the binding constant of $H^{14}CO_3^-$ to the Photosystem II complex in maize chloroplasts: Effects of inhibitors and light. Photochem Photobiol 38:101–707

Stemler A and Murphy JB (1985) Bicarbonate-reversible and irreversible inhibition of Photosystem II by monovalent anions. Plant Physiol 77: 974–977

Stiehl HH and Witt HT (1969) Quantitative treatment of the function of plastoquinone in photosynthesis. Z Naturforsch 24c: 1588–1598

Stowell MHB, McPhillips TM, Rees DC, Soltis SM, Abresch E and Feher G (1997) Light-induced structural changes in photosynthetic reaction center — implications for mechanism of electron-proton transfer. Science 276: 812–816

Sundby C, Chow WS and Anderson JM (1993) Effects on Photosystem I1 function, photoinhibition, and plant performance of the spontaneous mutation of serine 264 in the Photosystem I1 reaction center D1 protein in triazine-resistant *Brassica napus* L. Plant Physiol 103: 105–113

Tang X-S, Peloquin JM, Lorigan GA, Britt RD and Diner BA (1995) The binding environment of the reduced primary quinone electron acceptor Q_A of PS II. In: Mathis P (ed) Photosynthesis: From Light to Biosphere, Vol I, pp 775–778. Kluwer Academic Publishers, Dordrecht

Taoka S (1989) Kinetics of electron transfer and binding of inhibitors in the two-electron gate of chloroplasts. PhD Thesis, University of Illinois at Urbana-Champaign

Taoka S and Crofts AR (1987) Competition of Inhibitors with the secondary quinone in dark-adapted thylakoid membranes. In: Biggins J (ed) Progress in Photosynthesis Research Vol 2, pp 425–428, Martinus Nijhoff / Dr W Junk Publishers, The Hague

Taoka S and Crofts AR (1990) Two-electron gate in triazine resistant and susceptible *Amaranthus hybridus.* In: Baltscheffsky M (ed) Current Research in Photosynthesis, Vol I, pp 547–550. Kluwer Academic Publishers, Dordrecht

Taoka S, Robinson HH and Crofts AR (1983) Kinetics of the reactions of the two-electron gate of Photosystem II: Studies on the competition between plastoquinone and inhibitors. In Inoue Y, Crofts AR, Govindjee, Murata N, Renger G and Satoh K (eds) The Oxygen Evolving System of Photosynthesis, pp 369–381. Academic Press, Tokyo

Tietjen KG, Draber W, Goossens J, Jansen JR, Kluth JF, Schindler M, Wroblowsky H-J, Hilp U and Trebst A (1993) Binding of triazines in the Q_B-binding niche of Photosystem II. Z Natur-

forsch 48c: 205–212
Trebst A (1986) The topology of the plastoquinone and herbicide binding peptides of Photosystem II in the thylakoid membrane. Z Naturforsch 41c: 240–245
van Gorkom HJ (1996) Electroluminescence. Photosynth Res 48: 107–116
van Mieghem F, Nitschke W, Mathis P and Rutherford AW (1989) The influence of the quinone-iron electron acceptor complex on the reaction centre photochemistry of Photosystem II. Biochim Biophys Acta 977: 207–214
van Rensen JJS (2002) Role of bicarbonate at the acceptor side of Photosystem II. Photosynth Res 73: 185–192
van Rensen JJS, Tonk WJM and de Bruijn SM (1988) Involvement of bicarbonate in the protonation of the secondary quinone electron acceptor of Photosystem II via the non-haem iron of the quinone iron acceptor complex. FEBS Lett 226: 347–351
van Rensen JJS, Xu CH and Govindjee (1999) Role of bicarbonate in Photosystem II, the water-plastoquinone oxidoreductase of plant photosynthesis. Physiol Plant 105: 585–592
Vass I and Govindjee (1996) Thermoluminescence from the photosynthetic apparatus. Photosynth Res 48: 117–126
Velthuys BR (1976) Charge accumulation and recombination in system 2 of photosynthesis. PhD Thesis, Rijksuniversiteit te Leiden
Velthuys BR (1981) Electron-dependent competition between plastoquinone and inhibitors for binding to Photosystem II. FEBS Lett. 126: 277–281
Velthuys BR (1982) The function of plastoquinone in electron transfer. In: Trumpower BL (ed) Function of Quinones in Energy-Conserving Systems, pp 401–408. Academic Press, New York
Vermaas WFJ and Rutherford AW (1984) EPR measurements on the effects of bicarbonate and triazine resistance in the acceptor side of Photosystem II. FEBS Lett 175: 243–248
Vermaas WFJ, Renger G and Arntzen CJ (1989) Herbicide/quinone interactions in photosystem 11. Z Naturforsch 139c: 368–373
Vernotte C, Briantais JM, Astier C, Govindjee (1993) Differential effects of formate in single and double mutants of D1 in *Synechocystis* PCC 6714. Biochim Biophys Acta 1229: 296–301
Wraight CA (1979) Electron acceptors of bacterial photosynthetic reaction centers. Biochim Biophys Acta 548: 309–327
Wraight CA (1981) Oxidation-reduction physical chemistry of the acceptor quinone complex in bacterial photosynthetic reaction centers: Evidence for a new model of herbicide activity. Isr J Chem 21: 348–354
Wraight CA (1985) Modulation of herbicide-binding by the redox state of Q_{400}, an endogenous component of Photosystem II. Biochim Biophys Acta 809: 320–330
Wraight CA (2004) Proton and electron transfer in the acceptor quinone complex of photosynthetic reaction centers from *Rhodobacter sphaeroides.* Frontiers in Biosciences 9: 309–337
Xiong J, Hutchison RS, Sayre RT, Govindjee (1997) Modification of the Photosystem II acceptor side function in a D1 mutant (arginine-269-glycine) of *Chlamydomonas reinhardtii*. Biochim Biophys Acta 1322: 60–76
Xiong J, Subramaniam S and Govindjee (1998a) A knowledge based 3-D model of the Photosystem II reaction center of *Chlamydomonas reinhardtii*. Photosynthesis Research 56: 229–254
Xiong J, Minagawa J, Crofts A, Govindjee (1998b) Loss of inhibition by formate in newly constructed Photosystem II D1 mutants, D1-R257E and D1-R257M, of *Chlamydomonas reinhardtii*. Biochim Biophys Acta 1365: 473–491
Yoshida S, Oettmeier W and Boger P (1993) Proceedings of International Workshop on Chloroplast Metabolism and its Inhibition by Herbicides, Saitama, Japan, 1992. Z Naturforsch 48c: 119–405
Zheng M, and Dismukes GC (1996) The Conformation of the isoprenyl chain relative to the semiquinone head in the primary electron acceptor (Q_A) of higher plant PS II (plastosemiquinone) differs from that in bacterial reaction centers (ubisemiquinone or menasemiquinone) by ca. 90°. Biochemistry 35: 8955–8963
Zimmermann J-L and Rutherford AW (1986) Photoreductant-induced oxidation of Fe^{2+} in the electron acceptor complex of Photosystem II. Biochim Biophys Acta 851: 416–423
Zouni A, Witt H-T, Kern J, Fromme P, Krauß N, Saenger W and Orth P (2001) Crystal structure of Photosystem II from *Synechococcus elongatus* at 3.8 Å resolution. Nature 409: 739–743